Zircon geochronology of bottom rocks in the central Arctic Ocean: analytical results and some geological implications

Garrik Grikurov[1], Oleg Petrov[2], Sergey Shokalsky[2], Pavel Rekant[1], Alexey Krylov[1,4], Anatoly Laiba[3], Boris Belyatsky[1,2], Mikhail Rozinov[2] and Sergey Sergeev[2,4]

[1]I.S. Gramberg Research Institute for Geology and Mineral Resources of the World Ocean 'VNIIOkeangeologia', 1Angliysky Ave., 190121 St. Petersburg, Russia
[2]A.P. Karpinsky Russian Research Geological Institute 'VSEGEI', 74 Sredny Prospect, 199106 St. Petersburg, Russia
[3]Polar Marine Geosurvey Expedition, 24 Pobedy St., 188512 Lomonosov – St. Petersburg, Russia
[4]St. Petersburg State University,7/9 Universitetskaya Emb., 199034 St. Petersburg, Russia

ABSTRACT

In the past few years sampling of deepwater seabed gained an increasingly important role in studying geological structure of the Arctic Ocean. A common concept of virtually uninterrupted pelagic drape in the Amerasia Basin and exclusively ice-rafted nature of all clastic components that occur in bottom sediments was challenged by recent discoveries of bedrock exposures in the sea floor, while correlation of results of analytical study of bottom samples collected by the Russian expeditions in 2000, 2005 and 2007 with bathymetric environments at respective sites suggested that certain dredged and cored coarse rock fragments appeared meaningful for bedrock characterization if even the source sub-pelagic outcrop was not positively documented. The first results of age determinations of detrital zircons that were extracted from coarse fragments of lithic sedimentary rocks resting on the seabed and in the immediate sub-bottom, as well as of zircons from fragments of magmatic/metamorphic rocks and of zircon grains separated directly from sub-pelagic unlithified sediments are in agreement with published interpretations of the Lomonosov Ridge bedrock as composed of Mesozoic terrigenous sequences; the presence of an older Neoproterozoic(?) – Early-Middle Paleozoic basement is also possible. The Mendeleev Rise bedrock, too, is believed to mainly consist of Paleozoic-Early(?) Mesozoic sedimentary superstructure that may locally rest on the Earliest Paleozoic or even older units. Basaltic rocks likely to originate from the High Arctic Large Igneous Province (HALIP) has not so far been found among the collected fragments but limited loose zircon grains probably derived from broadly contemporaneous magmatic products were recorded in sub-pelagic sediment along with dropstones of variably metamorphosed Precambrian mafic and granitoid rocks.

INTRODUCTION

Great progress in acquisition of new bathymetric and geophysical data relevant to understanding the geological structure and history of the Arctic Ocean, including the tectonic nature of enigmatic Central-Arctic bathymetric highs, was achieved in recent years by the Arctic countries through their programs for delineation of respective extended continental shelves. However, only limited direct geological information was obtained on the composition of sub-bottom bedrock concealed by almost continuous drape of young sediments. Only at a few sites can the lithic fragments recovered by bottom sampling be interpreted with sufficient confidence as representing *in situ* submarine bedrock, while in most cases they are regarded ice rafted debris (IRD) of questionable derivation.

In search of provenance of lithic and mineral clastic components in bottom sediments we conducted age determinations on zircon crystals of two categories: (1) extracted from the rock fragments and (2) separated directly from hemipelagic sediments. In this paper we present the results of more than 700 zircon U-Pb age measurements completed before 2012. The samples labeled AF00, AF05, AF07 were collected during MS "Akademik Fedorov" cruises Arctic-2000, 2005, 2007, those marked ALR07 were acquired in 2007 on board NIB (nuclear icebreaker) "Rossiya", and two specimens designated BC were selected for the analysis from clastic material sampled by RV "Polarstern" in the course of ARK-XXIII/3-2008 cruise.

Sampling sites were located on Mendeleev Rise, Lomonosov Ridge, on deep Amundsen Basin seabed at the North Pole, and on the bathyal floor in the southern Podvodnikov Basin (Fig 1). Dredging equipment used during Arctic-2000 expedition was supplemented by box and gravity coring on the Arctic-2005 cruise, whereas RV “Polarstern” and the Arctic-2007 cruises employed different types of coring but did not execute any dredging. Sampling on RV “Polarstern” was controlled by Parasound observations which indicated a continuous presence along the ship track of sub-bottom hemipelagic sediments at least several dozen meters thick (Jokat, 2009). Selection of sampling localities surveyed by Russian vessels was only guided by bathymetric data available at the time of cruises.

Zircon dating was performed by high-resolution SIMS method on SHRIMP-II instrument in the Centre of Isotopic Research at VSEGEI, St. Petersburg, Russia. Zircon grains of different morphologies were measured using regular analytical procedure similar to that described by Williams (1998, and references therein) and reference zircons Temora2 (for U/Pb ratios) and 91500 (for U content). Each analytical spot had size ca 2x20x25 µm.

DESCRIPTION OF ANALYZED MATERIAL

Zircons in fragments of magmatic and/or metamorphic rocks (Fig. 2)

Almost 200 age determinations, including:

- **Station/sample AF07-01 (North Pole)**: five semi-angular to semi-rounded gravel-pebble size fragments (0.5-0.6 – 1.5-2.0 cm) of granitic rocks with indistinct gneissic banding recovered from box cored pelagic mud. Zircons were analyzed by SIMS SHRIMP directly in thin sections (21 measurements).
- **Station ALR07-16**: steep western slope of the Geophysicists Spur. Box cored sediments with abundant small rock fragments of variable composition with unusually high proportions of metamorphic and igneous lithologies. Zircon grains were separated from three little splinters of fine-grained gneiss-like rocks and enabled 15 age determinations.
- **Station/sample BC-299**: Podvodnikov Basin.

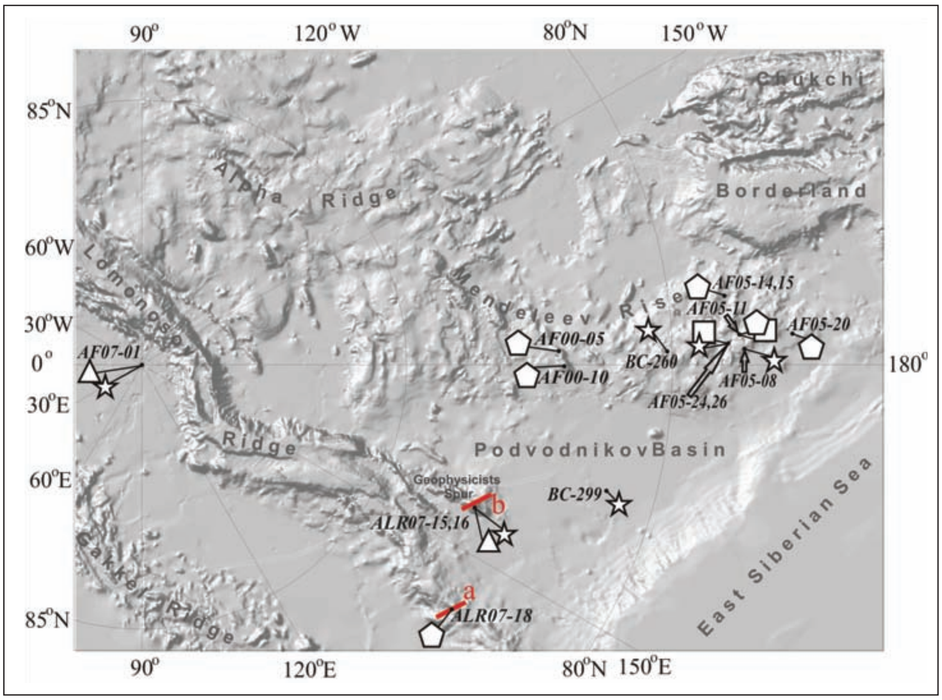

Fig. 1. Location of sampling sites described in this paper. Geological stations designated AF00, AF05 and AF07 were made from MS “Akademik Fedorov” in 2000, 2005 and 2007, respectively, ALR07 from NIB “Rossiya” in 2007, and BC from RV “Polarstern” in 2008. Specimens represented by large fragments and/or pebble-gravel sized debris of zircon-bearing rocks are marked by pentagons (sandstones, siltstones), stars (granitic and gneissic rocks) and squares (metagabbro-dolerites). Triangles indicate samples of hemipelagic sediments. Red lines correspond to the position of small sections of seismic lines shown in Fig. 6.

A single pebble-like fragment of plagiogranite over 2 cm in size from gravity cored sediment (12 U-Pb isotope analyses were made in thin section).

- **Stations/samples AF05-08, AF05-24, AF05-26** (dredges) and **BC-260** (box corer): southern Mendeleev Rise. Scarce fragments of muscovite, biotite and/or two-mica gneissoid granites and plagiogranites, often cataclastically deformed, gravel-pebble sized, semi-angular to semi-rounded at all sites. One specimen (AF05-08) with distinct gneissic banding had noticeably larger size (8-9 cm) and an almost non-abraded shape. Small pieces of regular petrographic thin sections (without cover glasses) containing visible zircon grains were implanted in standard SIMS mounts (over one hundred measurements).
- **Stations/samples AF05-11, AF05-26**: southern Mendeleev Rise, dredges. Three small fragments of metagabbro-dolerites among variable other lithologies (25 zircon age determinations in thin sections).

Detrital zircons extracted from fragments of quartz sandstones (Fig. 3)

Stations/samples AF00-05, 10, AF05-11, 14, 15, 20 – different parts of Mendeleev Rise, station/sample ALR07-18 – Lomonosov Ridge. Numerous sandstone fragments of highly variable size (usually from 1.5-2.0 cm to 10-15 cm, the largest is nearly 40 cm) were recovered by dredges, box and gravity corers and altogether enabled more than 300 zircon age determinations.

Detrital zircons in soft sediments

Station/sample AF07-01 – deepwater seabed at the North Pole, approximately 120 km from the foot of the Lomonosov Ridge. Small portions of soft sediments totaling ~ 300 grams in weight were arbitrary selected from the box cored sample, then mixed and reduced to heavy minerals concentrate which contained about 250 zircon grains. Approximately half of that number appeared unsuitable for age determination (grains too small, or fractured, or filled with inclusions). Unbroken crystals were picked out by hand and analyzed in grain mounts (103 age determinations).

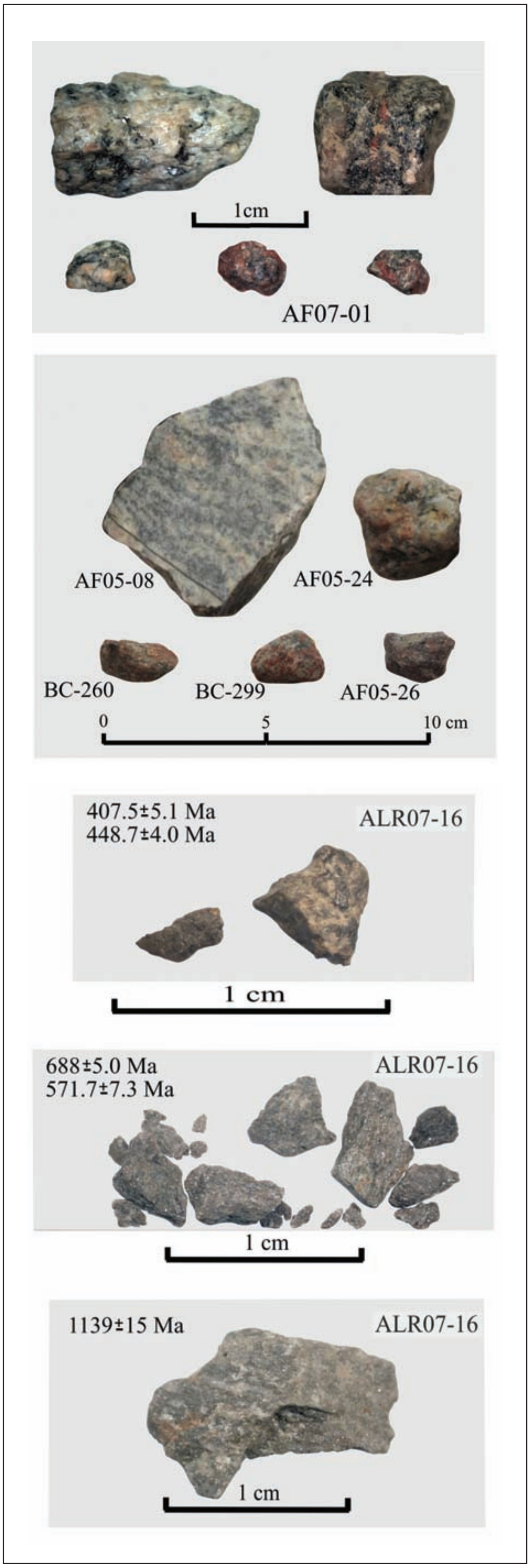

Fig. 2. Morphological appearance of granitoid rock fragments hosting magmatic zircons that were analyzed.

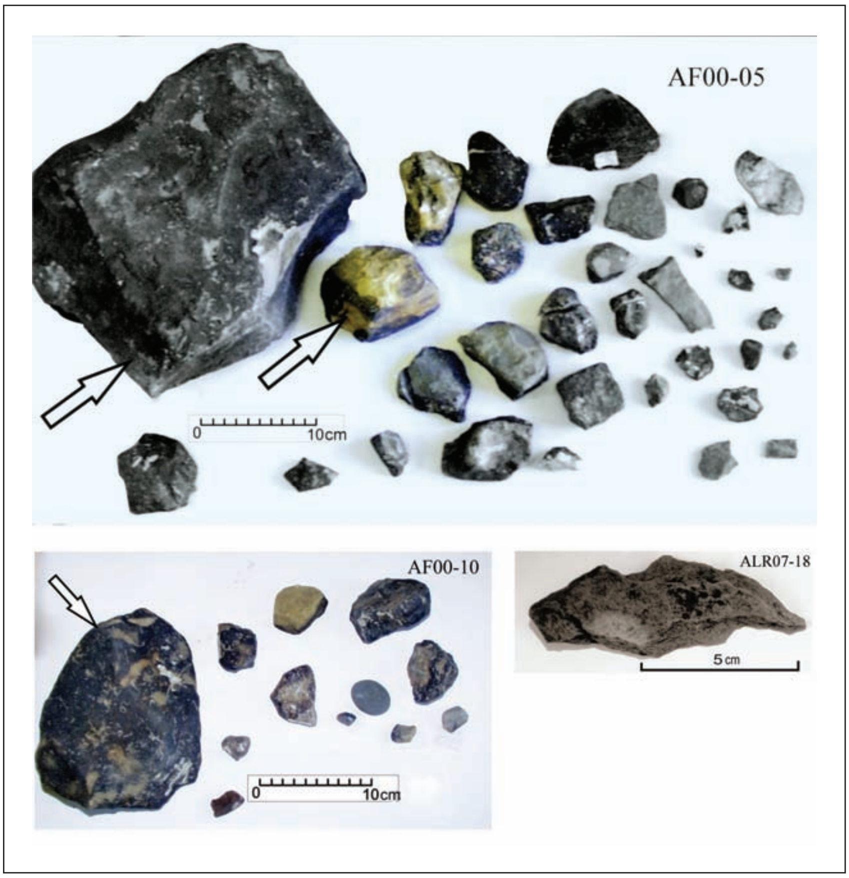

Fig. 3. Examples of the morphological appearance of sedimentary rocks fragments sampled. Arrows indicate the biggest of sandstone fragments dredged at stations AF00-05 & 10 (central Mendeleev Rise) that were selected for age determinations; other debris includes both terrigenous and carbonate rocks some of which are likely to represent IRD. Sandstone specimen ALR07-18 (southern Lomonosov Ridge) was retrieved by gravity core from 55 cm b.s.f.

Station/sample ALR07-15 – steep western slope of the Geophysicists Spur 3 km away from the station ALR07-16. A continuous sub-bottom succession was cored to 9 m below sea floor (b.s.f.) and sampled at ~1 m intervals, each sample up to 500 g in weight providing 200-300 small zircon grains. The first 152 measurements reported in this paper were performed on zircons from 12-14 cm b.s.f., 505-507 cm b.s.f. and 703-705 cm b.s.f. (ca 50 grain analyses for each sample).

SUMMARY OF ANALYTICAL RESULTS

The analytical data are presented in the annex (Tables 1 and 2) and illustrated in Figures 4-5. Only concordant or sub-concordant age data were considered for detrital zircons. A brief description of obtained zircon ages is given below.

Fig. 4 demonstrates the lack of apparent correlation between the ages and morphological characteristics of analyzed zircon grains.

Ages of detrital zircons extracted from fragments of sandstones (Fig. 5A):

A common feature of all analyzed specimens is the prevalence of zircons with ages mainly in ~2000 –1000 Ma interval (late Paleoproterozoic – Mesoproterozoic). Yet Precambrian zircons in samples AF00-05 and AF00-10 are mostly late Paleoproterozoic (~2000-1700 Ma), whereas the majority of grains in all other sandstones are Mesoproterozoic (~1800-1700 – 1000 Ma). Another peculiarity of AF00-05 & AF00-10 sandstones is the paucity of Archean zircons relative to the amount observed in other studied sandstones and in soft sediments.

One more distinctive feature of the AF00-05 and AF00-10 specimens is the dominating presence of zircons with Paleozoic to early Mesozoic U-Pb ages whose peaks on the histograms closely resemble the major clusters in hemipelagic sediments. In other sandstones zircons with such ages are absent or very poorly defined.

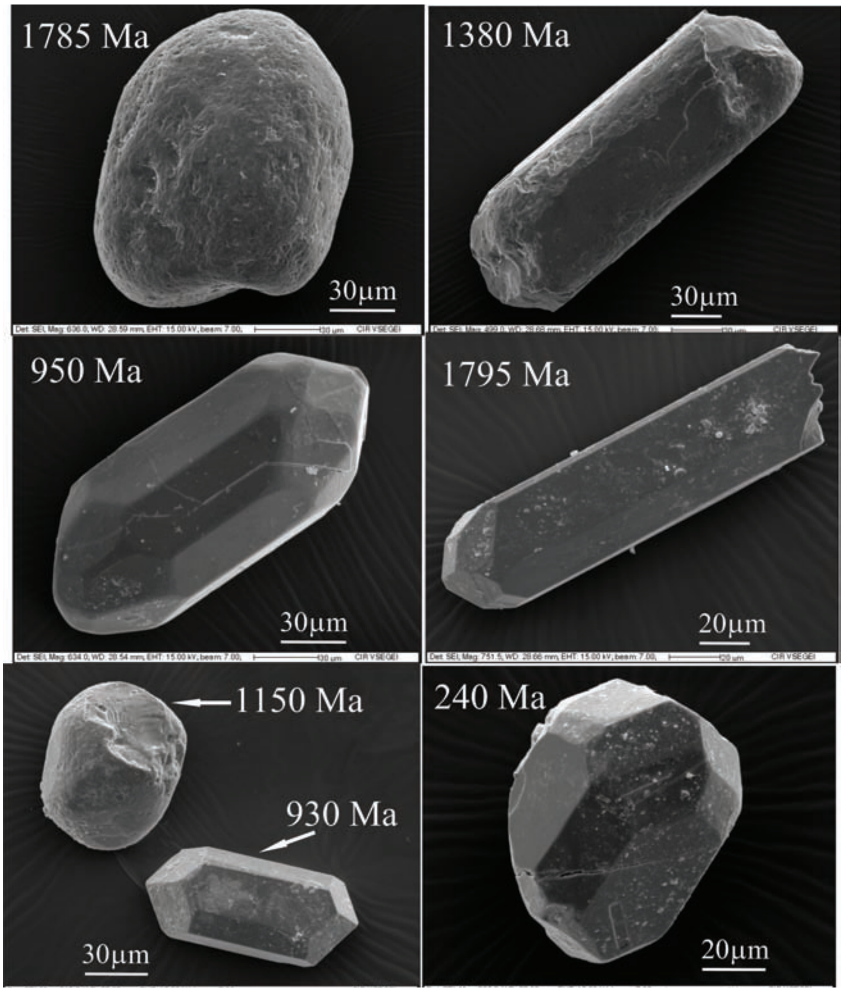

Fig. 4. Selected SE images of zircon crystals from sandstone specimens AF00-05 and AF00-10 showing lack of correspondence between measured U-Pb ages and the degree of grains roundness.

Ages of zircons in fragments of magmatic and metamorphic rocks (Fig. 5B):

Ages of zircons from granitoid fragments in samples AF07-01, AF05-08, AF05-24, AF05-26 and BC-299 suggest that all listed rocks were mainly crystallized in the Neoarchean (2600 – 2700 Ma). AF07-01 specimens additionally point to the possibility that the parental magma for these granitoids was derived from a Mesoarchean (ca. 2900 Ma) crustal source. Indications of Paleoproterozoic overprint are present in all granitoid samples. The largest and least rounded specimen AF05-08 with the most distinct gneissocity was probably also affected by the Latest Neoproterozoic metamorphic event, as suggested by the presence of rare 600-800 Ma zircon grains with secondary rims.

Granitic rock BC-260 contains only late Paleoproterozoic zircons.

The best estimated value of 790±20 Ma obtained on zircons from metagabbro-dolerite specimens AF05-11 and AF05-26 most likely represents the age of magmatic crystallization. Older values close to 2650 Ma and 1950 Ma are closely comparable to ages determined for the granitic rocks and may reflect the presence of zircons captured by mafic magma from older crustal material.

Zircons from three small fragments of gneiss-like rocks collected on Geophysicists Spur (ALR07-16) displayed ~1140 Ma, ~570-690 Ma ~400-450 Ma ages. The oldest age was obtained (single shot) on a sole grain recovered from one of the fragments; of three grains extracted from the second fragment two showed ~ 690 Ma (six shots), and one ~ 570 Ma (two shots); and two grains from the third splinter exhibited ~ 407 Ma and ~ 448 Ma ages (three measurements on each grain).

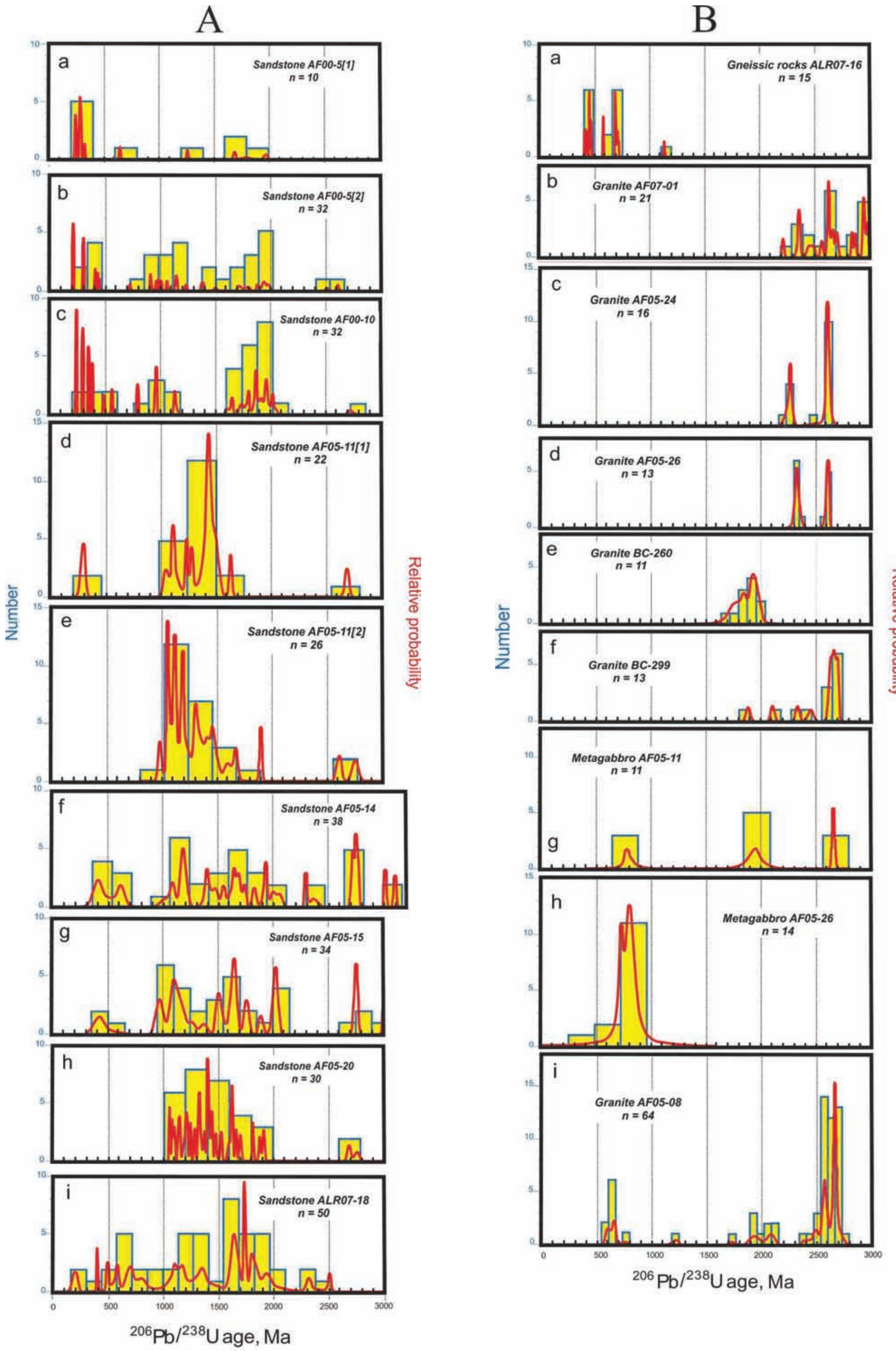
A
B
a
Sandstone AF00-5[1]
n = 10
b
Sandstone AF00-5[2]
n = 32
c
Sandstone AF00-10
n = 32
d
Sandstone AF05-11[1]
n = 22
e
Sandstone AF05-11[2]
n = 26
f
Sandstone AF05-14
n = 38
g
Sandstone AF05-15
n = 34
h
Sandstone AF05-20
n = 30
i
Sandstone ALR07-18
n = 50
Number
Relative probability
^{206}Pb/^{238}U age, Ma
a
Gneissic rocks ALR07-16
n = 15
b
Granite AF07-01
n = 21
c
Granite AF05-24
n = 16
d
Granite AF05-26
n = 13
e
Granite BC-260
n = 11
f
Granite BC-299
n = 13
g
Metagabbro AF05-11
n = 11
h
Metagabbro AF05-26
n = 14
i
Granite AF05-08
n = 64
Number
Relative probability
^{206}Pb/^{238}U age, Ma

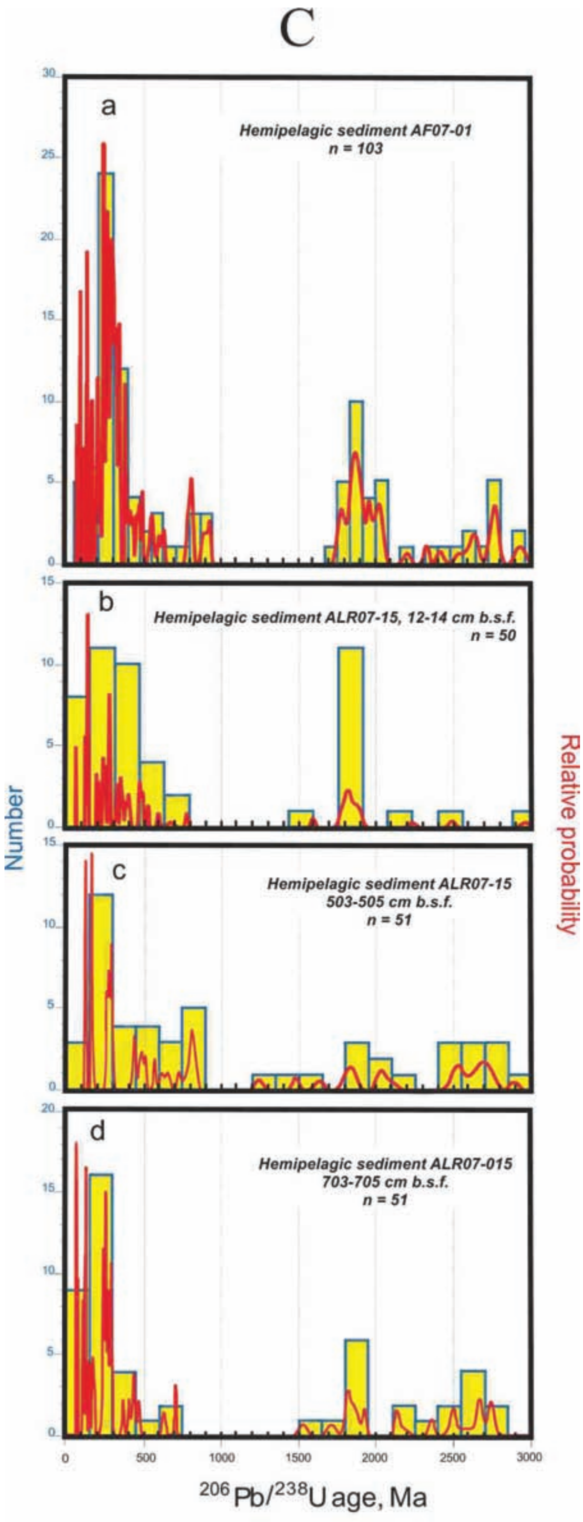

Fig. 5. Distribution of measured zircon ages. A – ages of detrital zircons in sandstone fragments, B – ages of zircons in metamorphosed magmatic rocks, C – ages of detrital zircons in sub-bottom sediments. See text for explanation.

Ages of detrital zircons in Recent sediments (Fig. 5C):

The majority of ages are younger than ~ 500 Ma (Phanerozoic) with lesser peaks in ~ 2000-1800 Ma age interval (late Paleoproterozoic). Neoproterozoc and Meso-Neoarchean determinations are subordinate. A distinct age gap is documented between ~ 1800 and 1000 Ma.

DISCUSSION

The presence of basement outcrops not concealed under sub-pelagic cover or accessible for sampling at shallow sub-bottom depth has been reported, with greater or lesser confidence, from several sites located on the Lomonosov Ridge (Grantz et al., 2001), the southern Northwind Ridge (Grantz et al., 1998), on the central and northern Northwind Ridge, seamounts between Alpha and Northwind Ridges and the southern Alpha Ridge (Andronikov et al., 2008; Brumley et al., 2010, 2011; Database for ECS Dredge Samples at NOAA/NGDC), and in the central Alpha Ridge (Clark et al., 2000; Jokat, 2003; Van Wagoner et al., 1986). The coarse debris that can positively be attributed to, or inferred to represent the bedrock, is usually mixed with variable proportions of IRD consisting mainly of quartz-rich terrigenous and carbonate rocks. This IRD was defined by Grantz et al. (2011a) as "… shallow marine Paleozoic carbonates and sandstones … widely distributed on the seabed of the Amerasia Basin by the basin's clockwise Beaufort Gyre current system"; the authors (ibid) further concluded that "…sedimentary clasts in the dredges and cores from Mendeleev Ridge belong to an areally extensive suite of glacial erratics that originated in NW Canada…" Our data suggest that such definition is probably excessively all-embracing, and at least some of the coarse clastic material in sampled bottom sediments on the Mendeleev Rise may appear meaningful for characterization of the local bedrock.

Rock specimens interpreted to represent sub-pelagic basement

The sandstone fragments bearing detrital zircons analyzed in the present study were collected in three different areas – the central Mendeleev Rise, the southern Mendeleev Rise and the near-Siberian segment of the Lomonosov Ridge (see pentagons in Fig. 1). These geographic variations are reflected in the distribution of detrital zircons ages and other characteristics of respective specimens (Fig. 5A).

The largest of all recovered sandstone fragments were dredged on a small, steep-sided bathymetric spur in the central Mendeleev Rise (sites AF00-05 & 10). Three fragments were analyzed and displayed only slightly differing zircon age data (Fig. 5A, a-c) notably dissimilar to those in the sandstones from the southern Mendeleev Rise. The marked distinctions of these data, such as well expressed Paleozoic-Early Mesozoic zircons population, prevalence of Paleoproterozoic ages over Mesoproterozoic determinations and almost total lack of Archean grains, suggest clastic input from the sources independent from those involved in formation of the sandstones dredged farther south. The central sites are also peculiar for the occurrence of fossiliferous Paleozoic limestones (Kaban'kov et al., 2004) not encountered elsewhere in the sampled area. In our view, these features are likely to signify that AF00-05 & 10 sandstone/carbonate debris represents local Paleozoic and Mesozoic (mostly pre-200 Ma?) sedimentary bedrock strata whose upper horizons may be broadly correlative with sub-pelagic basement of the Lomonosov Ridge described by Grantz et al. (2001) and exemplified in our collection by the specimen ALR07-18 discussed below.

A common feature of specimens from the southern Mendeleev Rise is the predominance of Mesoproterozoic detrital zircons (Fig. 5A, d-h). Sandstones AF05-11[2] and AF05-20 which contain only pre-1000 Ma grains can in reality be as old as Neoproterozoic; this may or may not also be true for the specimen AF05-11[1] where the ~ 200-400 Ma zircon ages are probably too rare to be meaningful. However, more numerous ~ 400-600 Ma grains in specimens AF05-14 & 15 (Fig. 5A, f-g) seem to preclude their Precambrian age; these sandstones also contain lesser amounts of Mesoproterozoic grains and a greater number of ancient grains, some of them as old as Mesoarchean.

Unless caused by the shortage of analytical data, such peculiarities may suggest that sandstones collected at stations 14, 15 and those recovered at stations 11 and 20 differ in age and origin, despite geographical proximity of these sites and apparent lithological similarity of the studied rocks. They also further confirm the dissimilarity of the southern and the central Mendeleev Rise specimens. If corroborated by subsequent studies, these distinctions would seem easier to explain by local derivation of the analyzed rocks than by their ice rafting from remote sources and selective unloading at different Mendeleev Rise locations. For instance, the presence of Archean grains captured in the analyzed sandstones indicates that these rocks could not be derived from the nearest coastal mainland - the Arctic Alaska-Chukotka (AAC) terrane which was shown by Akinin et al. (2012) to lack the Archean juvenile crust.

The Lomonosov Ridge specimen ALR07-18 is composed of coarse quartzose siltstone with carbonate cement. Zircon U-Pb age data (Fig. 5A, i) indicate input from sources ranging in age from Paleoproterozoic to possibly as young as Early Mesozoic. Except some clustering at about the Paleo/Mesoproterozoic boundary, the distribution of ages is relatively flat throughout more than a 2000 Ma time interval suggesting multiple recycling of primary clastic material. Lithological composition of the analyzed rock, its likely post-Triassic depositional age and detrital zircons population are consistent with the characterization of the Lomonosov Ridge bedrock by Grantz et al. (2001). The location of sampling site at the base of steep Lomonosov Ridge slope in close vicinity to the near-bottom high of the acoustic basement (Fig. 6a) and a sharply angular shape of the collected specimen suggest possibility of its derivation from a proximal submarine outcrop.

Among magmatic/metamorphic rock fragments the most likely representatives of bedrock were recovered by box corer at the Geophysicists Spur at site ALR07-16 (Fig. 1, Rekant et al., 2012). Here the unusual abundance of fragments is accompanied by uncommonly large amount (about 50%) of metamorphic rocks which at all other sampling sites are invariably markedly subordinate to unaltered carbonate and terrigenous clasts. Increase in overall concentration of coarse material could be caused by slumping of sediments and washing out of fine particles – the processes likely to occur on a steeply faulted slope (Fig. 6b); however, the remarkably high proportion of magmatic/metamorphic rock fragments is uncharacteristic of IRD and, when considered together with bathymetric profile at the sampling site, suggests supply from the local bedrock.

All box-cored rock splinters were too small for preparation of thin sections or chemical treatment. So far only three of them that could visually (using binocular microscope) be defined as gneisses of probable diorite composition were analyzed and showed different (~1140, ~570-690 and~400-450 Ma) ages. In the absence of detailed examination of the mineral composition, metamorphic grade, magmatic vs sedimentary origin, etc. of the samples studied, these ages could be interpreted as indicating that analyzed rocks belong to either the same polymetamorphic assemblage, or are derived from different metamorphic sources. The latter possibility, however, seems highly unlikely, since it would imply transportation of one piece from a Mezoproterozoic provenance, another from a Late Neoproterozoic terrane, and the third from an Early-Middle Paleozoic area. We therefore prefer the alternative option which allows correlation of the Geophysicists Spur bedrock with the basement assemblages reported from the Northwind Ridge (Brumley et al., 2010, 2011; Database for ECS Dredge Samples at NOAA/NGDC) and characterized by an ancient (no younger than Grenvillian) protolith affected by subsequent events as young as the Caledonian.

Rock fragments of questionable origin

Interpretation of mineral particles and/or relatively small rock pieces in bottom samples as IRD or otherwise relocated matter (e.g. Bischof et al., 1996; Clark et al., 1980; Grantz et al., 2011a; Phillips and Grantz, 2001) in all probability applies to those subordinate fragments in our collection which are characterized by predominantly small size, sub-rounded or pebble-like shape and, in some cases, display apparent association with glacial-dominated

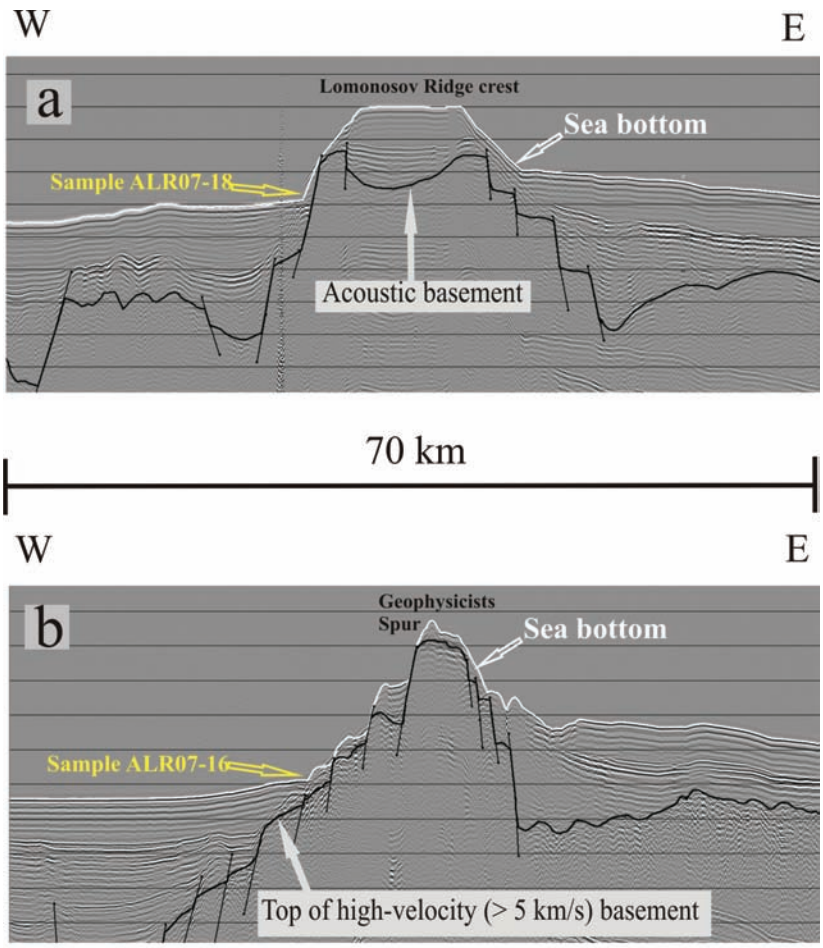

Fig. 6. Fragments of stacked seismic sections showing the position of sampling sites ALR07-18 (a) and ALR07-16 (b) relative to the bathymetry and basement behavior (modified from lines shot during Arctica-2011 cruise). Vertical exaggeration approximately 8:1. See Fig. 1 for the location of imaged sections.

layers in sub-bottom sediments. These features are inherent in the majority of analyzed magmatic rocks, namely the granitic pieces AF07-01, AF05-24 & 26, BC-260 & 299 and metagabbro-dolerites AF05-11 & 26 (Figs. 2 and 5B, b-h) which are therefore interpreted as dropstones of questionable origin.

Specimen AF05-08 (Figs. 2 and 5B, i) is distinct among granitoid rocks being much larger with pronounced gneissic banding and almost unsmoothed shape. Its zircon population is characterized by higher amount of Late Archean zircons and the presence of 600-800 Ma grains with secondary rims suggesting Latest Neoproterozoic overprint. The combination of these features may indicate the provenance more proximal than the source area of other Archean granitoids.

Mineral grains interpreted as IRD

Detrital zircons from soft bottom sediments have so far been studied in only two samples collected on different flanks of the Lomonosov Ridge (stations AF07-01 & ALR07-15, Figs. 1 and 5C). Ages of zircons selected at different levels from the ALR07-15 core appeared barely distinguishable (Fig. 5C, b-d). This can either be attributed to invariability of sources that supplied zircon grains to the sampling site during the time spanned by the cored interval, or may merely reflect intermixing of loose sediments on a steep slope. Other findings attracting attention in Fig. 5C are (1) general similarity of zircon age data obtained in radically diverse geographical and geomorphological environments – site AF07-01 in deepwater Amundsen basin (Fig. 5C, a) vs. site ALR07-15 on a prominent bathymetric spur (Fig. 5C, b-d), (2) presence at both localities of post-Triassic grains not recorded in any of the analyzed rock fragments, and (3) notable absence of Mesoproterozoic zircons which constitute the most characteristic population in the studied sandstone specimens.

The first two observations can be interpreted as signifying either a common source or separate but closely comparable provenances. The latter would at first glance seem represented by proximal Paleozoic-Mesozoic sedimentary bedrock reportedly sampled on the Lomonosov Ridge (Grantz et al., 2001) and, based on interpretation of our zircon data from sandstone specimens, also thought to occur on the Mendeleev Rise, at least in the vicinity of sampling sites in the central part. However, upon closer examination such explanation appears difficult to accept. For the North Pole site it would be hard to imagine how abundant heavy mineral products eroded from the Lomonosov Ridge sedimentary bedrock could be delivered to the sampling locality across more than 100 km of flat deepwater Amundsen Basin, and in case of the Geophysicist Spur our data suggest that the bedrock here is more likely composed of Late Precambrian-Early Paleozoic metamorphic basement than of younger rocks capable of releasing post-500 Ma zircons into pelagic sediment.

Ice rafted zircons in sub-pelagic sediments appear therefore the most likely possibility, if even the light minerals and clay components in these deposits could be supplied to both sampling localities by turbidity currents from a variety of sources, including as distal ones as the Laptev Sea shelf. As shown by Krylov et al. (2008) on the basis of ACEX data, in post-Middle Miocene time zircon was a steady component (6-8%) of the heavy minerals assemblage continuously delivered to the Lomonosov Ridge and adjacent bathymetric deeps by Transpolar ice drift from the Arctic margin of Eastern Asia. Consequently, the Phanerozoic and Neoproterozoic zircons could easily be derived from various geological formations of respective age mapped in this extensive region. The provenance of Early Precambrian zircons is more problematic. They could either be supplied from the same enigmatic shield sources which gave rise to the above mentioned magmatic/metamorphic dropstones, or assumed to originate from younger igneous rocks containing inherited ancient grains that were captured by parental melts.

The youngest detrital zircons in Recent sub-bottom sediments are Late Cretaceous. In all probability they mostly originate from HALIP and/or broadly contemporaneous volcanic products which are exposed on the Circum-Arctic mainland and islands (Akinin and Miller, 2012; Korago et al., 2010) and believed to extend throughout much of the central Arctic Ocean (e.g. Grantz et al., 2011b). However, based on geophysical data the near-Pole to Russia segment of the Lomonosov Ridge is commonly excluded from the area affected by Late Mesozoic volcanic activity and therefore can hardly serve as a local source for zircons of that age. This further strengthens the notion of their distal derivation and ice rafted nature

The virtual absence in modern deposits of Mesopoterozoic zircons indicates that mineral grains in pelagic sediments were not recycled from sandstones disseminated on the seabed. In case of such recycling the zircon population in sub-bottom layers would be dominated by Precambrian rather than Phanerozoic ages.

CONCLUSIONS

Intensification in recent years of bottom sampling in the central Arctic Ocean was accompanied by implementation of improved methods of site control and state-of-the-art analytical studies of the collected material. This enabled more exact examination of the nature of recovered bottom specimens and expanded the opportunities for interpretation of their lithological and age characteristics in regional geological context.

Our zircon geochronological data suggest that the sandstone/carbonate fragments dredged on the central Mendeleev Rise at sites AF00-05 & 10 most likely represent local Paleozoic and Mesozoic (mainly pre-200 Ma?) sedimentary bedrock units. The youngest of the central Mendeleev Rise sandstones may be broadly correlative with sub-pelagic Mesozoic sedimentary bedrock of the Lomonosov Ridge confirmed by sampling near the North Pole (Grantz et al., 2001) and believed to be exemplified in the Pole to Siberia segment of the ridge by our specimen ALR07-18 of coarse quartzose siltstone.

The presence of post-500 Ma sandstones among the samples from the southern Mendeleev Rise is more questionable, since the analyzed specimens from this area provided so far only a much lower number of zircons younger than 1000 Ma. At the same time, the well expressed population in these rocks of Mesoproterozoic grains is not a sufficient argument in favor of derivation of the analyzed sandstones from local Neoproterozoic bedrock, as assumed by Kaban'kov et al. (2004, 2008, 2012). While not ruled out by the available data, such possibility requires a much stronger confirmation. Distribution of Precambrian grains in detrital zircon population from Cambrian quartzites in the Canadian Arctic (Hadlari et al., 2012) is very similar to that observed in our specimens of quartzose sandstones from the southern Mendeleev Rise. Consequently, the latter are not necessarily Neoproterozoic and may also be Cambrian or younger, and until their inferred local provenance is constrained with better confidence, the derivation of these rocks from the Canadian provenance and transportation by ice to the Mendeleev Rise will be difficult to disprove.

Zircon geochronology of sandstone debris in bottom sediments from the Mendeleev Rise and the Lomonosov Ridge suggests that these submarine highs are largely underlain by Paleozoic-Early Mesozoic sedimentary bedrock. The latter may in places include Early-Middle Paleozoic fold basement, but the predominance of younger (Middle Paleozoic to Early Mesozoic) platform-type or transitional sequences seems a more likely possibility.

Limited evidence for the presence of older assemblages is provided at the Geophysicists Spur basement high interpreted to consist of metamorphic rocks of possible Grenville-Caledonian affinity.

The source of variably metamorphosed Late Precambrian mafic and Archean granitoid rocks interpreted as dropstones is uncertain. One of many probabilities is that during the glacial maximum they could be scoured by ice from the shallowest blocks of the Lomonosov Ridge some of which may, by analogy with the plateau described by Jackson and Dalh_Jensen et al. (2010), be composed of ancient(?) high-velocity crystalline infrastructure virtually uncovered by sediments.

On the whole, the preliminary geological implications of the present study are consistent with the models proposing significant extension of mature continental crust as a leading mechanism of formation of the Amerasia Basin (Miller et al., 2006; Laverov et al., 2013).

ACKNOWLEDGEMENTS

We thank Dr. Vyacheslav Akinin and anonymous reviewer for constructive comments which highlighted the parts of the text that lacked adequate clarity and prompted respective revisions helping to improve the paper. Participation of A. Krylov in laboratory studies of the bottom samples was partly supported by the RFBR grant 12-05-00364-a.

Table 1. U-Pb SHRIMP-II analytical data.

Analysis number	% $^{206}Pb_c$	ppm U	ppm Th	ppm $^{206}Pb^*$	$^{232}Th/^{238}U$	(1) $^{206}Pb/^{238}U$ Age (Ma) ± abs		(1) $^{207}Pb/^{206}Pb$ Age (Ma) ± abs		% Dis.	(1) $^{238}U/^{206}Pb^*$	±%	(1) $^{207}Pb^*/^{206}Pb^*$	±%	(1) $^{207}Pb^*/^{235}U$	±%	(1) $^{206}Pb^*/^{238}U$	±%	err corr
Hemipelagic sediments from the North Pole site, sample AF07-01 (89°59'10.9"N, 32°19'13.8")																			
79.1	0.00	128	82.3	1.47	0.66	85.2	2.3	286	213	235	75.17	2.7	0.0520	9.3	0.095	9.7	0.0133	2.7	0.28
91.1	0.64	2121	613	30.6	0.30	107	1.0	116	123	9	59.98	1.0	0.0483	5.2	0.111	5.3	0.0167	1.0	0.18
34.1	0.00	126	133	2.24	1.09	132	2.7	672	133	408	48.29	2.1	0.0619	6.2	0.177	6.6	0.0207	2.1	0.31
52.1	0.00	276	105	5.43	0.39	146	2.0	128	98	-12	43.64	1.4	0.0486	4.2	0.154	4.4	0.0229	1.4	0.31
57.1	0.45	488	147	9.78	0.31	148	1.6	80	144	-46	43.01	1.1	0.0476	6.1	0.153	6.2	0.0232	1.1	0.17
27.1	0.00	68.6	52.7	1.62	0.79	175	4.1	126	245	-28	36.31	2.4	0.0485	10	0.184	11	0.0275	2.4	0.22
26.1	0.00	488	1487	11.9	3.15	181	2.4	171	81	-5	35.06	1.3	0.0495	3.5	0.195	3.7	0.0285	1.3	0.36
39.1	0.00	220	102	6.40	0.48	214	3.4	202	96	-6	29.57	1.6	0.0502	4.1	0.234	4.4	0.0338	1.6	0.36
1.1	1.38	893	421	27.0	0.49	220	3.0	270	216	22	28.78	1.4	0.0516	9.4	0.247	9.5	0.0347	1.4	0.14
18.1	0.00	33.2	39.3	1.00	1.22	222	8.0	343	238	54	28.49	3.7	0.0533	11	0.258	11	0.0351	3.7	0.33
12.1	0.00	37.0	58.9	1.16	1.64	231	6.7	284	224	23	27.38	3.0	0.0520	9.8	0.262	10	0.0365	3.0	0.29
30.1	0.00	323	220	11.0	0.70	250	3.4	231	83	-7	25.32	1.4	0.0508	3.6	0.277	3.9	0.0395	1.4	0.36
9.1	0.00	479	157	16.6	0.34	255	3.4	252	75	-1	24.75	1.4	0.0512	3.2	0.285	3.5	0.0404	1.4	0.39
44.1	0.02	775	899	27.0	1.20	256	3.3	259	59	1	24.70	1.3	0.0514	2.5	0.287	2.9	0.0405	1.3	0.45
47.1	1.11	100	177	3.53	1.82	256	5.7	69	303	-73	24.69	2.3	0.0474	13	0.265	13	0.0405	2.3	0.18
45.1	0.00	53.4	143	1.86	2.77	256	6.1	157	184	-39	24.68	2.4	0.0492	7.9	0.275	8.2	0.0405	2.4	0.30
99.1	0.00	612	418	21.5	0.71	258	2.6	288	54	11	24.46	1.0	0.0521	2.4	0.293	2.6	0.0409	1.0	0.39
2.1	0.00	35.6	67.7	1.30	1.97	268	8.6	586	233	118	23.53	3.3	0.0595	11	0.349	11	0.0425	3.3	0.29
93.1	0.58	338	216	12.6	0.66	272	3.3	156	149	-43	23.17	1.2	0.0492	6.4	0.293	6.5	0.0432	1.2	0.19
49.1	1.51	78.2	84.8	2.99	1.12	276	6.8	403	329	46	22.81	2.5	0.0548	15	0.331	15	0.0438	2.5	0.17
31.1	1.41	114	105	4.35	0.95	277	5.2	134	353	-52	22.81	1.9	0.0487	15	0.294	15	0.0438	1.9	0.13
46.1	0.60	172	175	6.52	1.06	278	4.6	228	164	-18	22.72	1.7	0.0507	7.1	0.308	7.3	0.0440	1.7	0.23
75.1	0.00	68.5	73.5	2.62	1.11	281	6.3	566	146	102	22.48	2.3	0.0590	6.7	0.362	7.1	0.0445	2.3	0.32
55.1	0.83	172	405	6.66	2.44	282	3.9	113	157	-60	22.33	1.4	0.0483	6.7	0.298	6.8	0.0448	1.4	0.21
42.1	0.78	144	165	5.59	1.19	283	4.9	235	198	-17	22.25	1.8	0.0509	8.6	0.315	8.7	0.0449	1.8	0.20
51.1	1.01	95.5	110	3.85	1.19	293	5.8	328	245	12	21.52	2.0	0.0530	11	0.339	11	0.0465	2.0	0.19
95.1	0.37	167	162	6.85	1.00	299	4.5	198	170	-34	21.08	1.5	0.0501	7.3	0.327	7.5	0.0474	1.5	0.21
68.1	2.43	52.9	82.1	2.21	1.60	299	7.9	-131	752	-144	21.08	2.7	0.0436	30	0.285	31	0.0474	2.7	0.09
87.1	0.70	142	54.1	5.91	0.39	303	5.0	222	189	-26	20.81	1.7	0.0506	8.2	0.335	8.3	0.0481	1.7	0.20
89.1	0.39	172	93.7	7.20	0.56	306	4.5	318	164	4	20.60	1.5	0.0527	7.2	0.353	7.4	0.0485	1.5	0.21
21.1	0.44	410	367	17.3	0.93	308	4.1	250	122	-19	20.44	1.4	0.0512	5.3	0.345	5.5	0.0489	1.4	0.25
19.1	0.00	63.0	80.9	2.69	1.33	312	6.9	286	153	-8	20.14	2.3	0.0520	6.7	0.356	7.1	0.0496	2.3	0.32
17.1	0.18	698	228	29.8	0.34	312	3.9	305	67	-2	20.14	1.3	0.0525	2.9	0.359	3.2	0.0497	1.3	0.40
15.1	0.00	372	88.7	16.0	0.25	316	4.8	287	81	-9	19.93	1.6	0.0520	3.5	0.360	3.9	0.0502	1.6	0.40
6.1	0.00	112	56.1	4.87	0.52	319	6.3	385	133	21	19.74	2.0	0.0543	5.9	0.379	6.2	0.0507	2.0	0.33
92.1	0.27	568	437	25.0	0.80	321	3.1	340	73	6	19.58	1.0	0.0533	3.2	0.375	3.4	0.0511	1.0	0.30
16.1	0.00	252	202	11.2	0.83	325	5.1	370	90	14	19.34	1.6	0.0540	4.0	0.385	4.3	0.0517	1.6	0.37
40.1	0.34	486	162	22.0	0.35	330	4.3	308	104	-7	19.04	1.3	0.0525	4.6	0.380	4.8	0.0525	1.3	0.28
22.1	0.00	337	533	15.3	1.63	333	4.5	361	65	9	18.89	1.4	0.0538	2.9	0.392	3.2	0.0529	1.4	0.43
38.1	0.68	128	124	5.92	1.00	335	5.6	373	194	11	18.72	1.7	0.0541	8.6	0.398	8.8	0.0534	1.7	0.20
33.1	0.00	387	267	18.0	0.71	339	4.4	294	66	-13	18.51	1.3	0.0522	2.9	0.389	3.2	0.0540	1.3	0.42
76.1	0.39	614	92.1	29.5	0.15	349	3.4	801	63	129	17.96	1.0	0.0658	3.0	0.505	3.2	0.0557	1.0	0.32
88.1	0.21	362	216	17.6	0.62	355	3.2	356	72	0	17.68	0.9	0.0536	3.2	0.418	3.3	0.0566	0.9	0.28
7.1	0.00	206	122	10.0	0.61	355	5.3	362	88	2	17.67	1.5	0.0538	3.9	0.420	4.2	0.0566	1.5	0.37
14.1	0.78	192	92.2	9.47	0.50	357	5.7	332	194	-7	17.54	1.6	0.0531	8.6	0.417	8.7	0.0570	1.6	0.19
58.1	0.08	1365	2762	73.9	2.09	394	2.9	359	36	-9	15.88	0.7	0.0537	1.6	0.466	1.8	0.0630	0.7	0.43
48.1	0.44	213	90.3	11.7	0.44	397	5.8	416	116	5	15.72	1.5	0.0551	5.2	0.483	5.4	0.0636	1.5	0.28
81.1	0.00	86.5	64.1	4.80	0.77	403	8.4	380	117	-6	15.49	2.2	0.0542	5.2	0.483	5.7	0.0646	2.2	0.38
11.1	0.65	262	185	15.3	0.73	422	6.2	395	171	-6	14.80	1.5	0.0546	7.6	0.509	7.8	0.0676	1.5	0.19
25.1	0.00	179	119	10.8	0.69	440	6.6	436	74	-1	14.16	1.6	0.0556	3.3	0.542	3.7	0.0706	1.6	0.42
63.1	0.61	92.6	53.1	6.03	0.59	468	6.4	485	161	4	13.27	1.4	0.0568	7.3	0.591	7.4	0.0754	1.4	0.19
71.1	0.45	279	33.8	18.8	0.13	483	5.5	400	124	-17	12.84	1.2	0.0547	5.6	0.587	5.7	0.0779	1.2	0.21
97.1	0.00	666	362	46.3	0.56	501	4.3	469	34	-6	12.37	0.9	0.0564	1.6	0.629	1.8	0.0809	0.9	0.50
54.1	0.86	43.2	55.6	3.40	1.33	560	11.1	491	209	-12	11.01	2.1	0.0570	9.5	0.713	9.7	0.0908	2.1	0.21
86.1	0.00	44.1	32.4	3.49	0.76	568	12.3	596	128	5	10.85	2.3	0.0598	5.9	0.760	6.3	0.0921	2.3	0.36
78.1	1.74	112	65.9	9.78	0.61	613	9.7	382	272	-38	10.03	1.7	0.0543	12	0.746	12	0.0997	1.7	0.14
8.1	0.00	372	308	33.4	0.86	642	7.9	631	46	-2	9.554	1.3	0.0608	2.1	0.877	2.5	0.1047	1.3	0.52
28.1	0.24	114	28.4	12.9	0.26	796	11	766	75	-4	7.607	1.5	0.0648	3.6	1.173	3.9	0.1314	1.5	0.39
29.1	0.00	46.3	40.6	5.35	0.91	814	14	902	91	11	7.430	1.9	0.0691	4.4	1.282	4.8	0.1346	1.9	0.39
94.1	0.00	62.1	51.6	7.19	0.86	815	13	768	77	-6	7.419	1.7	0.0648	3.7	1.204	4.0	0.1348	1.7	0.42
98.1	0.00	271	66.8	31.6	0.26	822	8.0	765	39	-7	7.352	1.0	0.0647	1.9	1.214	2.1	0.1360	1.0	0.49
24.1	0.25	244	238	31.2	1.01	892	13	870	56	-2	6.739	1.6	0.0680	2.7	1.392	3.1	0.1484	1.6	0.50
5.1	0.00	114	47.7	14.9	0.43	915	14	864	63	-6	6.553	1.6	0.0679	3.0	1.428	3.4	0.1526	1.6	0.47
65.1	0.00	231	37.7	31.0	0.17	936	8.8	935	35	0	6.398	1.0	0.0702	1.7	1.513	2.0	0.1563	1.0	0.51
80.1	0.00	330	183	72.5	0.57	1469	13	1753	18	19	3.908	1.0	0.1072	1.0	3.784	1.4	0.2559	1.0	0.70
32.1	0.06	343	237	86.4	0.72	1658	19	1784	19	8	3.409	1.3	0.1091	1.0	4.410	1.7	0.2933	1.3	0.79
13.1	0.05	466	99.0	121	0.22	1707	18	1793	15	5	3.299	1.2	0.1096	0.8	4.581	1.5	0.3032	1.2	0.82
84.1	0.00	333	94.0	89.6	0.29	1755	15	1853	17	6	3.195	1.0	0.1133	0.9	4.888	1.4	0.3129	1.0	0.72
53.1	0.08	185	133	50.6	0.74	1779	15	1852	20	4	3.147	0.9	0.1132	1.1	4.961	1.4	0.3177	0.9	0.65
73.1	0.23	82.9	34.1	23.4	0.42	1830	22	1852	34	1	3.045	1.4	0.1133	1.9	5.128	2.3	0.3284	1.4	0.58
10.1	0.07	399	151	113	0.39	1836	20	1847	20	1	3.035	1.3	0.1129	1.1	5.130	1.7	0.3295	1.3	0.76
43.1	0.05	135	52.6	39.0	0.40	1863	23	1873	27	1	2.984	1.4	0.1146	1.5	5.294	2.1	0.3351	1.4	0.69
37.1	0.08	227	112	65.6	0.51	1865	21	1856	19	0	2.981	1.3	0.1135	1.1	5.250	1.7	0.3354	1.3	0.78
74.1	0.00	126	58.3	36.3	0.48	1870	19	1847	24	-1	2.972	1.2	0.1129	1.4	5.241	1.8	0.3365	1.2	0.66
100.1	0.00	154	81.6	44.7	0.55	1870	18	1891	22	1	2.971	1.1	0.1157	1.2	5.370	1.6	0.3366	1.1	0.67
10.2	0.36	82.8	23.8	24.0	0.30	1871	32	1858	39	-1	2.970	2.0	0.1136	2.2	5.274	2.9	0.3367	2.0	0.68
85.1	0.00	172	229	50.1	1.37	1882	18	1860	26	-1	2.950	1.1	0.1137	1.4	5.316	1.8	0.3390	1.1	0.60
83.1	0.03	1397	118	410	0.09	1893	13	1881	9	-1	2.929	0.8	0.1151	0.5	5.418	1.0	0.3414	0.8	0.84
82.1	0.01	218	238	64.5	1.13	1905	17	1897	19	0	2.908	1.0	0.1161	1.0	5.504	1.5	0.3438	1.0	0.70
77.1	0.05	257	211	76.4	0.85	1913	15	1925	15	1	2.894	0.9	0.1179	0.8	5.619	1.2	0.3455	0.9	0.72
36.1	0.21	218	45.5	65.5	0.22	1930	22	1950	20	1	2.863	1.3	0.1196	1.1	5.757	1.7	0.3491	1.3	0.76
56.1	0.00	88.6	54.2	27.0	0.63	1958	19	1933	24	-1	2.818	1.1	0.1184	1.3	5.796	1.8	0.3549	1.1	0.65
60.1	0.15	1346	20.6	412	0.02	1963	12	1918	8	-2	2.809	0.7	0.1175	0.5	5.767	0.9	0.3561	0.7	0.84
50.1	0.19	305	53.8	93.7	0.18	1967	22	1968	18	0	2.801	1.3	0.1208	1.0	5.943	1.6	0.3568	1.3	0.79
90.1	0.14	429	304	135	0.73	2005	15	2000	14	0	2.742	0.9	0.1230	0.8	6.183	1.2	0.3647	0.9	0.74
23.1	0.00	106	48.4	33.4	0.47	2009	27	2015	38	0	2.734	1.5	0.1241	2.1	6.256	2.6	0.3658	1.5	0.59
69.1	0.00	346	148	110	0.44	2032	16	2006	14	-1	2.698	0.9	0.1234	0.8	6.306	1.2	0.3706	0.9	0.76
4.1	0.27	81.6	26.3	26.1	0.33	2033	30	2055	40	1	2.698	1.7	0.1269	2.3	6.484	2.8	0.3707	1.7	0.60
66.1	0.00	162	58.2	51.7	0.37	2039	18	2035	19	0	2.688	1.0	0.1254	1.1	6.434	1.5	0.3721	1.0	0.70
3.1	0.05	280	274	98.4	1.01	2209	27	2174	16	-2	2.447	1.5	0.1357	0.9	7.649	1.7	0.4087	1.5	0.84
77.2	0.08	662	348	248	0.54	2332	16	2366	16	1	2.295	0.8	0.1518	0.9	9.120	1.3	0.4358	0.8	0.66

Table 1. Continued.

Analysis number	% $^{206}Pb_c$	ppm U	ppm Th	ppm $^{206}Pb^*$	$^{232}Th/^{238}U$	(1) $^{206}Pb/^{238}U$ Age (Ma)	± abs	(1) $^{207}Pb/^{206}Pb$ Age (Ma)	± abs	% Dis.	(1) $^{238}U/^{206}Pb^*$	±%	(1) $^{207}Pb^*/^{206}Pb^*$	±%	(1) $^{207}Pb^*/^{235}U$	±%	(1) $^{206}Pb^*/^{238}U$	±%	err corr
41.1	0.00	1026	307	401	0.31	2419	24	2376	7	-2	2.196	1.2	0.1527	0.4	9.583	1.3	0.4553	1.2	0.94
72.1	0.27	85.3	69.1	35.4	0.84	2537	27	2529	22	0	2.073	1.3	0.1671	1.3	11.11	1.8	0.4824	1.3	0.70
35.1	0.09	122	203	52.5	1.72	2609	30	2646	15	1	2.004	1.4	0.1793	0.9	12.33	1.7	0.4988	1.4	0.84
20.1	0.05	401	116	174	0.30	2634	26	2740	30	4	1.981	1.2	0.1897	1.8	13.21	2.2	0.5048	1.2	0.54
61.1	0.08	164	53.2	71.7	0.34	2651	22	2678	13	1	1.966	1.0	0.1827	0.8	12.82	1.3	0.5087	1.0	0.78
96.1	0.12	419	107	191	0.26	2739	19	2823	9	3	1.889	0.9	0.1996	0.5	14.57	1.0	0.5294	0.9	0.84
67.1	0.32	101	15.5	46.5	0.16	2761	27	2755	18	0	1.870	1.2	0.1915	1.1	14.12	1.6	0.5346	1.2	0.74
62.1	0.00	193	39.0	89.2	0.21	2770	20	2728	10	-2	1.863	0.9	0.1884	0.6	13.94	1.1	0.5368	0.9	0.81
60.2	0.00	151	50.0	70.1	0.34	2780	23	2906	12	5	1.854	1.0	0.2101	0.7	15.62	1.2	0.5392	1.0	0.81
59.1	0.00	412	281	191	0.70	2783	18	2701	10	-3	1.852	0.8	0.1853	0.6	13.79	1.0	0.5398	0.8	0.79
70.1	0.00	46.9	25.7	23.2	0.57	2938	37	2902	21	-1	1.732	1.6	0.2095	1.3	16.68	2.0	0.5773	1.6	0.76
64.1	0.15	51.0	34.5	25.3	0.70	2938	31	2936	17	0	1.732	1.3	0.2139	1.1	17.03	1.7	0.5773	1.3	0.78
Hemipelagic sediments from the Lomonosov Ridge (Geophysicists Spur), sample ALR07-15 (83° N, 156°E), 12-14 cm b.s.f.																			
49.1	2.37	360	154	3.51	0.44	72.8	1.4	-428	10	118	88.11	1.9	0.0388	30	0.061	30	0.0113	1.9	0.06
50.1	0.43	695	218	12.3	0.32	131	1.5	5	150	-2525	48.57	1.1	0.0461	6.0	0.131	6.1	0.0206	1.1	0.18
46.1	--	1046	521	19.3	0.51	137	1.4	226	180	40	46.48	1.1	0.0507	4.1	0.150	4.2	0.0215	1.1	0.25
31.1	0.58	430	662	8.38	1.59	145	1.6	143	174	-1	44.08	1.1	0.0489	7.4	0.153	7.5	0.0227	1.1	0.15
9.1	0.00	199	129	3.90	0.67	145	2.6	170	137	17	43.86	1.8	0.0495	5.9	0.156	6.1	0.0228	1.8	0.29
20.1	0.00	385	98.5	7.66	0.26	148	2.3	159	104	8	43.17	1.6	0.0492	4.5	0.157	4.7	0.0232	1.6	0.33
8.1	3.13	203	92.3	4.19	0.47	148	4.1	375	854	153	42.96	2.8	0.0541	38	0.173	38	0.0233	2.8	0.07
26.1	0.14	1204	381	24.1	0.33	148	1.7	164	68	11	42.94	1.1	0.0493	2.9	0.158	3.1	0.0233	1.1	0.37
32.1	0.00	507	139	13.9	0.28	202	2.4	205	56	1	31.38	1.2	0.0502	2.4	0.221	2.7	0.0319	1.2	0.45
33.1	--	172	86.6	4.97	0.52	214	2.9	518	174	60	29.64	1.4	0.0577	7.9	0.268	8.1	0.0337	1.4	0.17
2.1	1.14	160	109	5.36	0.70	244	4.8	189	303	-22	25.92	2.0	0.0499	13	0.265	13	0.0386	2.0	0.15
15.1	1.08	373	187	12.6	0.52	245	3.8	246	300	0	25.77	1.6	0.0511	13	0.273	13	0.0388	1.6	0.12
17.1	1.99	131	159	4.60	1.26	253	5.1	204	255	-19	25.00	2.1	0.0502	11	0.277	11	0.0400	2.1	0.18
13.1	0.66	1566	675	55.5	0.45	259	2.7	231	98	-11	24.39	1.0	0.0508	4.3	0.287	4.4	0.0410	1.0	0.24
11.1	0.00	42.8	47.8	1.63	1.15	280	7.4	357	194	28	22.52	2.7	0.0537	8.6	0.329	9.0	0.0444	2.7	0.30
25.1	0.84	542	686	20.9	1.31	281	3.5	242	151	-14	22.45	1.3	0.0510	6.5	0.313	6.7	0.0445	1.3	0.19
27.1	1.40	200	399	7.84	2.06	284	5.1	398	331	40	22.20	1.8	0.0547	15	0.339	15	0.0450	1.8	0.12
29.1	0.88	605	520	23.8	0.89	286	3.4	263	134	-8	22.07	1.2	0.0515	5.8	0.322	6.0	0.0453	1.2	0.20
38.1	0.00	527	327	20.6	0.64	287	3.0	299	44	4	21.96	1.1	0.0523	1.9	0.328	2.2	0.0455	1.1	0.48
3.1	0.00	17.1	28.1	0.77	1.69	329	15.1	1868	147	468	19.09	4.7	0.1143	8.2	0.825	9.4	0.0524	4.7	0.50
21.1	0.50	525	526	23.9	1.03	331	3.9	520	83	57	18.95	1.2	0.0577	3.8	0.420	4.0	0.0528	1.2	0.31
1.1	0.43	536	682	26.2	1.32	355	4.2	438	89	23	17.67	1.2	0.0556	4.0	0.434	4.2	0.0566	1.2	0.29
7.1	0.00	75.6	117	3.78	1.61	365	7.2	495	121	36	17.18	2.0	0.0571	5.5	0.458	5.8	0.0582	2.0	0.35
42.1	1.54	71.4	38.7	3.57	0.56	365	8.8	330	570	-11	17.16	2.5	0.0530	25	0.426	25	0.0583	2.5	0.10
30.1	0.37	283	277	15.2	1.01	389	5.2	409	102	5	16.07	1.4	0.0549	4.5	0.471	4.7	0.0622	1.4	0.29
10.1	0.68	318	410	17.8	1.33	403	5.0	322	151	-20	15.50	1.3	0.0528	6.7	0.470	6.8	0.0645	1.3	0.19
5.1	2.50	181	95.2	10.5	0.54	412	7.4	343	413	-17	15.13	1.9	0.0533	18	0.486	18	0.0660	1.9	0.10
16.1	0.91	174	170	11.5	1.01	475	7.9	594	270	25	13.08	1.7	0.0597	12	0.629	13	0.0764	1.7	0.14
34.1	0.29	410	183	27.0	0.46	476	5.0	386	93	-24	13.06	1.1	0.0544	4.1	0.574	4.3	0.0766	1.1	0.26
22.1	1.41	130	62.1	8.94	0.49	490	8.4	479	287	-2	12.66	1.8	0.0567	13	0.617	13	0.0789	1.8	0.14
14.1	0.36	512	90.7	35.2	0.18	494	5.6	460	80	-7	12.55	1.2	0.0562	3.6	0.617	3.8	0.0796	1.2	0.31
41.1	--	317	317	23.3	1.03	529	5.9	693	55	25	11.70	1.2	0.0625	2.6	0.737	2.8	0.0855	1.2	0.42
12.1	1.22	248	296	20.8	1.23	595	8.2	521	209	-12	10.34	1.4	0.0578	9.5	0.770	9.6	0.0967	1.4	0.15
40.1	0.19	414	73.6	39.1	0.18	673	24	1480	27	57	9.088	3.8	0.0926	1.4	1.405	4.0	0.1100	3.8	0.93
47.1	0.00	307	146	33.6	0.49	774	8.6	771	30	-0	7.843	1.2	0.0649	1.4	1.141	1.9	0.1275	1.2	0.64
4.1	0.32	926	150	224	0.17	1591	14	1919	16	21	3.570	1.0	0.1176	0.9	4.537	1.3	0.2799	1.0	0.76
28.1	0.21	195	122	52.9	0.65	1770	19	1848	28	4	3.163	1.2	0.1130	1.5	4.924	2.0	0.3160	1.2	0.63
35.1	0.03	239	81.3	65.4	0.35	1786	18	1831	15	3	3.133	1.2	0.1120	0.8	4.927	1.4	0.3192	1.2	0.82
39.1	--	179	84.7	49.7	0.49	1805	20	1866	19	4	3.096	1.3	0.1141	1.0	5.083	1.6	0.3230	1.3	0.78
24.1	0.00	222	158	61.9	0.74	1813	19	1873	20	3	3.079	1.2	0.1146	1.1	5.130	1.6	0.3247	1.2	0.74
37.1	0.01	639	156	178	0.25	1815	17	1794	24	-1	3.075	1.0	0.1097	1.3	4.918	1.7	0.3252	1.0	0.62
19.1	0.14	1046	237	295	0.23	1828	16	1878	12	3	3.049	1.0	0.1149	0.7	5.193	1.2	0.3279	1.0	0.82
18.1	0.13	139	93.0	39.6	0.69	1843	22	1859	27	1	3.021	1.4	0.1137	1.5	5.188	2.1	0.3309	1.4	0.68
43.1	--	259	153	73.8	0.61	1847	19	1871	13	2	3.014	1.2	0.1144	0.7	5.235	1.4	0.3317	1.2	0.85
36.1	0.03	882	68.3	255	0.08	1872	16	1901	52	2	2.968	1.0	0.1163	2.9	5.404	3.1	0.3369	1.0	0.33
23.1	0.00	255	134	74.7	0.54	1890	19	1872	19	-1	2.936	1.2	0.1145	1.0	5.378	1.6	0.3406	1.2	0.75
48.1	0.00	192	143	56.7	0.77	1902	21	1883	15	-1	2.913	1.3	0.1152	0.9	5.453	1.6	0.3432	1.3	0.83
44.1	0.00	159	26.5	56.6	0.17	2237	25	2387	15	7	2.410	1.3	0.1537	0.9	8.790	1.6	0.4149	1.3	0.83
6.1	0.08	681	420	276	0.64	2491	21	2645	10	6	2.119	1.0	0.1791	0.6	11.65	1.2	0.4718	1.0	0.87
45.1	--	537	175	270	0.34	2969	26	2946	26	-1	1.710	1.1	0.2154	1.6	17.37	1.9	0.5849	1.1	0.56
Hemipelagic sediments from the Lomonosov Ridge (Geophysicists Spur), sample ALR07-15 (83° N, 156°E), 505-507 cm b.s.f.																			
10.1	0.30	1579	44.8	29.1	0.03	137	2.9	263	81	93	46.70	2.2	0.0515	3.5	0.152	4.1	0.0214	2.2	0.52
37.1	0.87	570	226	10.6	0.41	137	2.1	36	180	-73	46.45	1.5	0.0468	7.4	0.139	7.5	0.0215	1.5	0.20
18.1	0.74	1009	273	19.4	0.28	142	3.0	-52	160	-137	45.04	2.2	0.0451	6.6	0.138	6.9	0.0222	2.2	0.31
26.1	0.00	222	86.2	5.15	0.40	172	4.1	814	86	373	36.99	2.4	0.0662	4.1	0.247	4.8	0.0270	2.4	0.50
23.1	3.86	114	60.7	2.81	0.55	176	5.6	65	920	-63	36.10	3.2	0.0470	39	0.181	39	0.0277	3.2	0.08
43.1	0.00	1300	169	31.0	0.13	176	2.5	154	60	-13	36.08	1.5	0.0491	2.6	0.188	3.0	0.0277	1.5	0.49
4.1	1.30	374	684	9.21	1.89	180	4.2	-17	360	-109	35.33	2.4	0.0457	15	0.178	15	0.0283	2.4	0.16
2.1	2.61	177	371	4.50	2.17	183	4.9	-100	560	-155	34.66	2.7	0.0440	23	0.176	23	0.0289	2.7	0.12
8.1	0.42	822	1087	29.8	1.37	266	5.6	310	98	17	23.75	2.2	0.0526	4.3	0.305	4.8	0.0421	2.2	0.45
27.1	0.37	703	260	25.6	0.38	266	5.6	258	100	-3	23.70	2.1	0.0514	4.4	0.299	4.9	0.0422	2.1	0.44
30.1	0.44	225	275	8.65	1.26	281	6.4	152	200	-46	22.47	2.3	0.0491	8.5	0.301	8.9	0.0445	2.3	0.26
35.1	1.91	124	79.8	4.85	0.66	281	5.8	120	500	-57	22.44	2.1	0.0480	21	0.297	21	0.0446	2.1	0.10
14.1	0.00	125	105	4.78	0.87	282	7.7	1236	120	339	22.38	2.8	0.0816	6.0	0.503	6.6	0.0447	2.8	0.42
15.1	0.66	712	524	28.8	0.76	295	6.4	164	140	-44	21.37	2.2	0.0494	5.9	0.318	6.3	0.0468	2.2	0.35
31.1	0.24	631	1516	25.8	2.48	300	4.1	290	69	-3	21.03	1.4	0.0521	3.0	0.342	3.3	0.0476	1.4	0.42
3.1	2.68	94.5	36.5	4.02	0.40	303	9.0	-84	760	-128	20.77	3.0	0.0440	31	0.295	31	0.0481	3	0.10
28.1	4.17	442	361	19.1	0.84	304	7.1	125	400	-59	20.70	2.4	0.0485	17	0.323	17	0.0483	2.4	0.14
5.1	1.11	260	155	15.8	0.62	436	9.7	233	200	-47	14.27	2.3	0.0508	8.7	0.491	9.0	0.0700	2.3	0.25
47.1	0.00	254	250	15.6	1.02	445	6.9	407	66	-8	14.00	1.6	0.0549	2.9	0.541	3.4	0.0714	1.6	0.48
34.1	1.19	105	87.1	7.02	0.85	475	8.6	383	330	-19	13.06	1.9	0.0543	15	0.573	15	0.0765	1.9	0.13
46.1	0.24	296	152	20.2	0.53	492	7.5	547	61	11	12.61	1.6	0.0585	2.8	0.639	3.2	0.0793	1.6	0.49
40.1	0.30	250	41.4	17.8	0.17	512	7.3	518	72	1	12.10	1.5	0.0577	3.3	0.657	3.6	0.0826	1.5	0.41
44.1	1.54	945	589	76.2	0.64	570	7.9	574	97	1	10.81	1.5	0.0592	4.5	0.754	4.7	0.0924	1.5	0.31
29.1	1.24	120	128	10.5	1.10	614	14	308	240	-50	10.00	2.5	0.0525	11	0.724	11	0.1000	2.5	0.23
42.1	1.13	45.3	21.7	4.20	0.50	653	14	575	270	-12	9.380	2.2	0.0592	12	0.870	13	0.1066	2.2	0.17
17.1	0.68	199	113	20.4	0.59	722	15	680	100	-6	8.430	2.2	0.0622	4.7	1.017	5.2	0.1186	2.2	0.43
11.1	0.25	402	329	43.9	0.85	769	16	759	48	-1	7.890	2.2	0.0645	2.3	1.127	3.2	0.1267	2.2	0.69
39.1	0.00	167	124	18.9	0.77	800	11	835	37	4	7.570	1.5	0.0669	1.8	1.219	2.3	0.1322	1.5	0.64
25.1	0.56	271	96.7	31.2	0.37	804	17	1802	40	124	7.530	2.2	0.1102	2.2	2.017	3.1	0.1328	2.2	0.70
36.1	0.16	209	148	23.9	0.73	805	11	753	62	-7	7.520	1.5	0.0643	2.9	1.180	3.3	0.1330	1.5	0.45

Table 1. Continued.

Analysis number	% $^{206}Pb_c$	ppm U	ppm Th	ppm $^{206}Pb^*$	$^{232}Th/^{238}U$	(1) $^{206}Pb/^{238}U$ Age (Ma) ± abs		(1) $^{207}Pb/^{206}Pb$ Age (Ma) ± abs		% Dis.	(1) $^{238}U/^{206}Pb^*$	±%	(1) $^{207}Pb^*/^{206}Pb^*$	±%	(1) $^{207}Pb^*/^{235}U$	±%	(1) $^{206}Pb^*/^{238}U$	±%	err corr
41.1	0.15	191	242	22.6	1.31	831	12	792	40	-5	7.270	1.5	0.0655	1.9	1.243	2.4	0.1376	1.5	0.61
6.1	0.78	77.0	6.28	14.2	0.08	1246	28	1754	69	41	4.690	2.4	0.1073	3.8	3.150	4.5	0.2133	2.4	0.54
33.1	0.00	71.7	33.2	15.9	0.48	1482	22	1464	32	-1	3.868	1.6	0.0918	1.7	3.274	2.4	0.2585	1.6	0.70
20.1	0.11	564	314	140	0.58	1636	31	1908	100	17	3.460	2.2	0.1168	5.6	4.650	6.0	0.2889	2.2	0.36
24.1	0.30	275	162	77.0	0.61	1815	34	1853	25	2	3.073	2.1	0.1133	1.4	5.080	2.6	0.3252	2.1	0.84
12.1	0.15	516	198	145	0.40	1827	34	1845	16	1	3.050	2.1	0.1128	0.9	5.100	2.3	0.3277	2.1	0.92
50.1	0.00	100	53.5	28.8	0.55	1861	27	1788	31	-4	2.988	1.7	0.1093	1.7	5.040	2.4	0.3346	1.7	0.70
32.1	0.13	156	84.3	49.6	0.56	2029	25	1995	19	-2	2.702	1.4	0.1226	1.1	6.250	1.8	0.3699	1.4	0.80
1.1	0.10	551	305	177	0.57	2043	36	1993	12	-2	2.681	2.1	0.1225	0.7	6.300	2.2	0.3729	2.1	0.95
19.1	0.06	223	78.5	74.2	0.36	2109	39	2038	17	-3	2.584	2.2	0.1256	1.0	6.700	2.4	0.3870	2.2	0.92
22.1	0.11	221	89.4	91.2	0.42	2522	45	2678	13	6	2.088	2.2	0.1827	0.8	12.06	2.3	0.4790	2.2	0.94
38.1	0.02	529	203	218	0.40	2529	29	2605	23	3	2.081	1.4	0.1748	1.4	11.58	2.0	0.4805	1.4	0.71
9.1	0.35	154	95.4	63.8	0.64	2532	48	2641	29	4	2.076	2.3	0.1787	1.7	11.85	2.9	0.4810	2.3	0.80
7.1	0.16	178	101	76.4	0.59	2603	50	2654	14	2	2.009	2.3	0.1801	0.9	12.35	2.5	0.4970	2.3	0.94
16.1	0.01	285	159	126	0.58	2665	46	2682	10	1	1.953	2.1	0.1832	0.6	12.93	2.2	0.5120	2.1	0.96
13.1	0.03	444	372	196	0.86	2672	47	2724	9.3	2	1.947	2.1	0.1879	0.6	13.30	2.2	0.5140	2.1	0.97
48.1	0.00	236	127	106	0.56	2704	35	2693	16	0	1.919	1.6	0.1844	1.0	13.25	1.8	0.5212	1.6	0.86
21.1	0.00	187	103	84.3	0.57	2715	48	2724	12	0	1.909	2.2	0.1879	0.7	13.57	2.3	0.5240	2.2	0.95
49.1	0.00	226	235	103	1.08	2752	33	2727	11	-1	1.878	1.5	0.1882	0.7	13.82	1.6	0.5326	1.5	0.92
45.1	0.05	336	80.0	164	0.25	2896	34	2800	9.2	-3	1.763	1.4	0.1969	0.6	15.40	1.6	0.5672	1.4	0.93
Hemipelagic sediments from the Lomonosov Ridge (Geophysicists Spur), sample ALR07-15 (83° N, 156°E), 703-705 cm b.s.f.																			
18.2	0.47	832	473	9.17	0.59	82	1.5	236	190	189	78.30	1.9	0.0509	8.1	0.090	8.3	0.0128	1.9	0.23
18.1	1.60	636	503	7.22	0.82	83	1.7	80	310	-4	76.90	2.0	0.0476	13	0.085	13	0.0130	2.0	0.15
22.1	0.45	1078	802	12.9	0.77	89	1.6	-15	190	-117	72.00	1.8	0.0458	8.0	0.088	8.1	0.0139	1.8	0.22
19.1	0.73	281	287	4.69	1.06	123	2.5	155	200	26	51.80	2.1	0.0491	8.4	0.131	8.7	0.0193	2.1	0.24
26.1	2.02	513	101	9.01	0.20	128	2.6	258	310	102	50.00	2.0	0.0514	14	0.142	14	0.0200	2.0	0.15
4.1	0.28	1772	244	33.1	0.14	138	2.3	151	75	9	46.11	1.7	0.0491	3.2	0.147	3.6	0.0217	1.7	0.46
23.1	0.38	732	280	14.0	0.40	141	2.5	113	120	-20	45.08	1.8	0.0483	5.3	0.148	5.6	0.0222	1.8	0.32
33.1	0.40	521	141	10.2	0.28	145	1.5	123	130	-15	43.95	1.1	0.0485	5.4	0.152	5.5	0.0228	1.1	0.19
20.1	1.56	289	83.3	5.80	0.30	147	3.1	311	330	112	43.45	2.2	0.0526	15	0.167	15	0.0230	2.2	0.15
1.1	2.69	243	139	5.55	0.59	165	3.5	13	510	-92	38.63	2.2	0.0463	21	0.165	21	0.0259	2.2	0.10
16.1	0.00	252	113	6.20	0.46	182	3.7	214	99	17	34.85	2.1	0.0504	4.3	0.199	4.8	0.0287	2.1	0.44
14.1	1.67	205	62.5	5.41	0.31	192	4.2	-62	450	-133	33.14	2.2	0.0449	18	0.187	19	0.0302	2.2	0.12
34.1	3.79	155	58.6	5.39	0.39	246	5.1	-439	910	-278	25.64	2.1	0.0390	35	0.208	35	0.0390	2.1	0.06
41.1	1.41	508	318	17.4	0.65	248	2.6	295	250	19	25.46	1.1	0.0522	11	0.283	11	0.0393	1.1	0.10
48.1	4.08	73.1	146	2.58	2.06	249	7.9	459	800	84	25.38	3.2	0.0560	36	0.300	36	0.0394	3.2	0.09
21.1	1.02	247	408	8.78	1.71	259	5.0	92	250	-65	24.37	2.0	0.0479	11	0.271	11	0.0410	2.0	0.18
5.1	4.02	60.2	53.3	2.25	0.91	263	9.2	623	710	137	24.00	3.6	0.0610	33	0.350	33	0.0416	3.6	0.11
44.1	0.60	165	179	5.99	1.12	265	3.8	371	160	40	23.79	1.5	0.0540	6.9	0.313	7.1	0.0420	1.5	0.21
32.1	0.26	940	548	34.5	0.60	269	1.9	267	57	-1	23.43	0.7	0.0516	2.5	0.304	2.6	0.0427	0.7	0.28
17.1	1.54	233	272	8.78	1.21	272	5.5	-30	430	-111	23.16	2.1	0.0455	18	0.271	18	0.0432	2.1	0.12
39.1	0.49	447	588	17.2	1.36	280	2.6	275	120	-2	22.50	1.0	0.0518	5.1	0.317	5.1	0.0444	1.0	0.19
37.1	4.54	88.2	65.3	3.63	0.76	288	7.8	1183	600	311	21.90	2.8	0.0790	30	0.500	31	0.0456	2.8	0.09
11.1	1.07	133	177	5.36	1.38	293	6.1	322	250	10	21.49	2.1	0.0528	11	0.339	11	0.0465	2.1	0.19
8.1	1.77	501	669	20.7	1.38	298	5.4	292	190	-2	21.15	1.9	0.0522	8.4	0.340	8.6	0.0473	1.9	0.21
38.1	0.91	486	212	20.0	0.45	300	2.9	378	200	26	21.02	1.0	0.0542	8.7	0.355	8.8	0.0476	1.0	0.11
28.1	0.19	937	220	47.9	0.24	372	6.0	321	52	-14	16.85	1.6	0.0528	2.3	0.432	2.8	0.0594	1.6	0.59
3.1	0.19	875	1567	49.7	1.85	412	6.5	425	44	3	15.17	1.6	0.0553	2.0	0.503	2.6	0.0659	1.6	0.64
2.1	0.20	906	1702	54.6	1.94	436	6.9	386	58	-11	14.28	1.6	0.0544	2.6	0.525	3.1	0.0700	1.6	0.54
24.1	0.54	218	120	13.4	0.57	442	7.8	445	120	1	14.09	1.8	0.0558	5.2	0.546	5.5	0.0710	1.8	0.33
50.1	2.76	223	112	14.9	0.52	469	6.2	605	250	29	13.24	1.4	0.0600	12	0.625	12	0.0755	1.4	0.12
40.1	1.01	48.6	27.7	4.35	0.59	632	11	774	190	23	9.700	1.9	0.0650	9.2	0.923	9.4	0.1030	1.9	0.20
49.1	0.20	499	414	49.6	0.86	705	5.1	702	45	0	8.654	0.8	0.0628	2.1	1.001	2.2	0.1155	0.8	0.34
6.1	0.05	273	94.6	62.8	0.36	1529	24	1804	18	18	3.736	1.7	0.1103	1.0	4.070	2.0	0.2677	1.7	0.87
25.1	0.07	214	91.8	56.0	0.44	1713	25	1703	20	-1	3.284	1.7	0.1043	1.1	4.381	2.0	0.3045	1.7	0.84
31.1	0.20	226	66.5	63.1	0.30	1814	12	1801	21	-1	3.077	0.8	0.1101	1.1	4.933	1.4	0.3249	0.8	0.55
13.1	0.13	188	121	53.0	0.67	1824	27	1843	21	1	3.057	1.7	0.1127	1.2	5.080	2.0	0.3271	1.7	0.83
15.1	0.12	167	75.0	47.4	0.46	1832	27	1850	20	1	3.041	1.7	0.1131	1.1	5.130	2.0	0.3287	1.7	0.84
7.1	0.12	254	115	72.8	0.47	1855	27	1857	17	0	2.999	1.7	0.1135	1.0	5.219	1.9	0.3334	1.7	0.87
10.1	0.06	202	184	58.8	0.94	1877	27	1871	18	0	2.959	1.7	0.1144	1.0	5.330	1.9	0.3379	1.7	0.86
47.1	0.06	520	101	156	0.20	1926	11	1919	13	0	2.872	0.7	0.1175	0.7	5.642	1.0	0.3481	0.7	0.69
43.1	0.19	642	596	217	0.96	2132	14	2773	8.6	30	2.551	0.8	0.1936	0.5	10.46	0.9	0.3919	0.8	0.82
27.1	0.36	76.1	19.2	26.3	0.26	2169	35	2216	34	2	2.498	1.9	0.1391	2.0	7.670	2.7	0.4000	1.9	0.69
35.1	0.06	231	146	87.4	0.65	2356	17	2366	16	0	2.267	0.9	0.1518	0.9	9.230	1.3	0.4411	0.9	0.69
12.1	0.04	293	73.8	119	0.26	2493	34	2500	10	0	2.117	1.6	0.1643	0.6	10.69	1.7	0.4722	1.6	0.94
30.1	0.02	394	193	160	0.51	2496	15	2495	8.6	0	2.115	0.7	0.1638	0.5	10.68	0.9	0.4729	0.7	0.82
9.1	0.15	146	20.9	62.1	0.15	2583	36	2619	14	1	2.028	1.7	0.1764	0.9	11.99	1.9	0.4929	1.7	0.89
45.1	0.04	282	139	124	0.51	2660	19	2651	11	0	1.958	0.9	0.1798	0.7	12.66	1.1	0.5107	0.9	0.80
36.1	0.06	271	80.7	119	0.31	2667	16	2649	18	-1	1.951	0.7	0.1796	1.1	12.69	1.3	0.5124	0.7	0.55
29.1	0.07	146	103	65.4	0.73	2698	38	2717	19	1	1.923	1.7	0.1871	1.2	13.41	2.1	0.5198	1.7	0.83
42.1	0.12	251	168	114	0.69	2741	17	2748	12	0	1.887	0.8	0.1907	0.7	13.93	1.0	0.5298	0.8	0.73
46.1	0.34	156	120	71.2	0.80	2741	20	2756	18	1	1.884	0.9	0.1916	1.1	14.00	1.4	0.5300	0.9	0.63
Granitoid fragments from hemipelagic sediments at the North Pole site (measurements in thin sections), sample AF07-01 (89°59'10.9"N, 32°19'13.8")																			
2_1.1	0.27	214	192	99.8	0.92	nd	nd	2651	21	nd	nd	nd	0.1798	1.2	nd	nd	nd	nd	nd
3_1.1	0.65	141	92	62.8	0.67	nd	nd	2684	25	nd	nd	nd	0.1834	1.5	nd	nd	nd	nd	nd
3_2.1	0.67	692	313	294	0.47	nd	nd	2668	12	nd	nd	nd	0.1817	0.7	nd	nd	nd	nd	nd
4_1.1	-0.02	763	407	413	0.55	nd	nd	2943	7.3	nd	nd	nd	0.2149	0.5	nd	nd	nd	nd	nd
4_2.1	0.17	808	414	464	0.53	nd	nd	2976	10	nd	nd	nd	0.2193	0.6	nd	nd	nd	nd	nd
4_3.1	2.34	2190	802	1239	0.38	nd	nd	2571	11	nd	nd	nd	0.1714	0.7	nd	nd	nd	nd	nd
4_4.1	0.20	2411	711	801	0.30	nd	nd	2635	6.0	nd	nd	nd	0.1781	0.4	nd	nd	nd	nd	nd
4_4.2	0.03	3209	984	1552	0.32	nd	nd	2633	8.0	nd	nd	nd	0.1778	0.5	nd	nd	nd	nd	nd
4_4.3	0.39	554	148	218	0.28	nd	nd	2454	17	nd	nd	nd	0.1598	1.0	nd	nd	nd	nd	nd
4_5.1	0.80	1396	167	661	0.12	nd	nd	2709	10	nd	nd	nd	0.1862	0.6	nd	nd	nd	nd	nd
4_6.1	0.07	1341	223	732	0.17	nd	nd	2954	7.9	nd	nd	nd	0.2163	0.5	nd	nd	nd	nd	nd
4_6.2	0.07	1112	167	558	0.16	nd	nd	2950	9.2	nd	nd	nd	0.2159	0.6	nd	nd	nd	nd	nd
4_7.1	0.19	4328	294	1559	0.07	nd	nd	2370	8.7	nd	nd	nd	0.1521	0.5	nd	nd	nd	nd	nd
4_8.1	0.29	1533	286	608	0.19	nd	nd	2625	9.4	nd	nd	nd	0.1770	0.6	nd	nd	nd	nd	nd
4_8.2	0.06	1723	131	868	0.08	nd	nd	2871	8.1	nd	nd	nd	0.2056	0.5	nd	nd	nd	nd	nd
4_8.3	0.09	1984	1299	1131	0.68	nd	nd	2843	7.7	nd	nd	nd	0.2021	0.5	nd	nd	nd	nd	nd
4_9.1	0.07	1486	278	856	0.19	nd	nd	2987	8.2	nd	nd	nd	0.2209	0.5	nd	nd	nd	nd	nd
5_1.1	4.47	2846	1628	1361	0.59	nd	nd	2360	16	nd	nd	nd	0.1512	0.9	nd	nd	nd	nd	nd
5_2.1	2.33	1739	1277	867	0.76	nd	nd	2492	16	nd	nd	nd	0.1634	1.0	nd	nd	nd	nd	nd
5_3.1	0.04	2617	963	1271	0.38	nd	nd	2366	12	nd	nd	nd	0.1517	0.7	nd	nd	nd	nd	nd
5_4.1	0.07	4111	496	1812	0.12	nd	nd	2221	10	nd	nd	nd	0.1395	0.6	nd	nd	nd	nd	nd

Table 1. Continued.

Analysis number	% $^{206}Pb_c$	ppm U	ppm Th	ppm $^{206}Pb^*$	$^{232}Th/^{238}U$	(1) $^{206}Pb/^{238}U$ Age (Ma) ± abs		(1) $^{207}Pb/^{206}Pb$ Age (Ma) ± abs		% Dis.	(1) $^{238}U/^{206}Pb^*$	±%	(1) $^{207}Pb^*/^{206}Pb^*$	±%	(1) $^{207}Pb^*/^{235}U$	±%	(1) $^{206}Pb^*/^{238}U$	±%	err corr
Gneissic rocks from the Lomonosov Ridge (Geophysicists Spur), sample ALR07-16 (83.152° N, 156.105°E)																			
65_1.2	2.67	386	356	21.8	0.95	399	4.5	450	380	13	15.63	1.2	0.0560	8.8	0.493	8.9	0.0639	1.2	0.13
65_1.1	3.27	616	657	35.6	1.10	406	4.3	422	320	4	15.37	1.1	0.0552	7.4	0.495	7.5	0.0650	1.1	0.15
65_1.3	5.23	579	553	35.2	0.99	418	4.6	524	400	26	14.91	1.1	0.0578	9.2	0.534	9.3	0.0669	1.1	0.12
65_2.2	2.47	1572	663	99.2	0.44	446	3.4	532	160	19	13.96	0.8	0.0580	3.9	0.573	3.9	0.0716	0.8	0.20
65_2.3	3.07	1454	622	92.5	0.44	446	3.7	308	230	-31	13.93	0.9	0.0525	5.3	0.519	5.3	0.0717	0.9	0.16
65_2.1	1.38	1675	693	106	0.43	454	3.3	496	120	9	13.71	0.8	0.0571	2.7	0.574	2.8	0.0729	0.8	0.27
9_2.2	0.20	462	325	36.8	0.73	571	4.7	570	86	0	10.80	0.9	0.0591	2.0	0.754	2.2	0.0926	0.9	0.39
9_2.1	0.41	351	211	28.2	0.62	573	5.7	591	200	3	10.75	1.0	0.0597	4.7	0.765	4.8	0.0930	1.0	0.22
9_1.4	0.05	928	49.0	88.9	0.05	681	5.0	645	48	-5	8.972	0.8	0.0612	1.1	0.940	1.4	0.1115	0.8	0.57
9_1.2	0.00	864	27.2	82.8	0.03	682	5.0	702	39	3	8.961	0.8	0.0630	1.0	0.969	1.2	0.1116	0.8	0.62
9_1.1	0.08	704	749	67.7	1.10	684	5.2	682	53	0	8.938	0.8	0.0623	1.2	0.960	1.5	0.1119	0.8	0.55
9_3.2	1.45	126	57.8	12.4	0.47	692	9.2	653	340	-6	8.810	1.4	0.0614	8.0	0.960	8.2	0.1134	1.4	0.17
9_1.3	0.08	313	244	30.8	0.80	699	6.1	688	65	-2	8.734	0.9	0.0624	1.6	0.985	1.8	0.1145	0.9	0.50
9_3.1	0.23	149	63.2	14.9	0.44	708	7.7	679	120	-4	8.616	1.2	0.0621	2.9	0.994	3.1	0.1160	1.2	0.37
4_1.1	0.55	1049	347	175	0.34	1137	7.7	1160	46	2	5.180	0.7	0.0785	1.1	2.088	1.4	0.1929	0.7	0.54
Granitoid fragments from the Podvodnikov Basin, sample BC-299 (81°N, 165°E)																			
5_2.1	2.02	2322	321	416	0.14	1196	7.0	1872	19	57	4.907	0.7	0.1144	1.1	3.217	1.3	0.2038	0.7	0.52
5.1	0.80	573	77.9	143	0.14	1627	9.9	2085	17	28	3.483	0.7	0.1290	1.0	5.110	1.2	0.2871	0.7	0.58
7.1	1.15	1171	372	296	0.33	1643	9.1	2305	17	40	3.446	0.6	0.1464	1.0	5.862	1.2	0.2902	0.6	0.54
5_3.1	1.88	464	66.3	129	0.15	1765	12	2421	23	37	3.176	0.8	0.1566	1.3	6.810	1.6	0.3149	0.8	0.50
mica-5.1	0.95	765	407	277	0.55	2244	15	2615	17	17	2.402	0.8	0.1758	1.0	10.10	1.3	0.4164	0.8	0.60
mica-3.1	0.59	598	195	218	0.34	2267	13	2591	16	14	2.373	0.7	0.1734	1.0	10.08	1.2	0.4214	0.7	0.58
mica-4.1	0.14	502	134	186	0.28	2308	19	2585	16	12	2.323	1.0	0.1728	1.0	10.26	1.4	0.4304	1.0	0.71
6.2	0.89	972	133	367	0.14	2325	14	2652	11	14	2.303	0.7	0.1799	0.7	10.77	1.0	0.4342	0.7	0.73
7_2.1	0.28	619	285	238	0.48	2377	13	2596	13	9	2.243	0.7	0.1740	0.8	10.69	1.0	0.4458	0.7	0.65
6.1	0.08	577	47.6	232	0.09	2473	15	2637	16	7	2.138	0.7	0.1782	1.0	11.49	1.2	0.4677	0.7	0.60
6.3	0.38	696	364	282	0.54	2482	15	2659	10	7	2.129	0.7	0.1807	0.6	11.70	1.0	0.4696	0.7	0.76
7_3.1	0.50	415	157	170	0.39	2498	16	2622	13	5	2.113	0.8	0.1766	0.8	11.53	1.1	0.4733	0.8	0.70
mica-2.1	0.42	341	292	141	0.88	2515	16	2628	14	5	2.096	0.8	0.1774	0.8	11.67	1.2	0.4771	0.8	0.69
Granitoid fragments from the Mendeleev Rise, sample AF05-08 (78°40'N, 179°W)																			
1_12.1	1.74	91.0	49.7	7.39	0.56	573	13	644	244	12	10.76	2.4	0.0611	11	0.784	12	0.0929	2.4	0.21
1_15.1	1.47	84.8	72.5	6.99	0.88	583	15	529	318	-9	10.57	2.6	0.0580	14	0.756	15	0.0946	2.6	0.18
1_4.1	7.23	14.0	8.42	1.25	0.62	595	38	-127	2004	-121	10.34	6.6	0.0437	81	0.583	81	0.0967	6.6	0.08
1_13.1	0.99	120	140	10.3	1.20	604	13	513	243	-15	10.19	2.3	0.0576	11	0.779	11	0.0982	2.3	0.20
1_17.1	1.52	79.3	41.7	7.13	0.54	633	16	690	236	9	9.696	2.7	0.0625	11	0.888	11	0.1031	2.7	0.23
1_3.1	0.37	97.2	60.7	8.73	0.65	638	14	826	140	29	9.605	2.4	0.0666	6.7	0.956	7.1	0.1041	2.4	0.33
1_16.1	1.14	99.5	95.4	9.07	0.99	643	14	784	215	22	9.540	2.4	0.0653	10	0.944	11	0.1048	2.4	0.22
1_1.1	0.27	668	20.8	61.6	0.03	655	9.3	589	55	-10	9.345	1.5	0.0596	2.5	0.879	2.9	0.1070	1.5	0.51
1_10.1	3.53	39.0	17.7	4.22	0.47	740	31	581	967	-21	8.220	4.4	0.0594	45	0.996	45	0.1217	4.4	0.10
1_6.1	2.41	81.8	36.8	14.8	0.47	1208	27	953	256	-21	4.850	2.4	0.0709	13	2.015	13	0.2062	2.4	0.19
1_2.1	0.40	117	70.6	31.0	0.62	1724	30	1780	37	3	3.262	2.0	0.1088	2.0	4.600	2.8	0.3065	2.0	0.70
1_8.1	0.43	148	158	43.9	1.10	1904	30	1978	36	4	2.911	1.8	0.1215	2.0	5.754	2.7	0.3436	1.8	0.67
1_9.1	0.28	266	219	79.6	0.85	1922	27	2037	24	6	2.879	1.6	0.1256	1.4	6.015	2.1	0.3474	1.6	0.76
1_26.1	1.70	95.7	96.4	29.5	1.04	1945	38	2038	71	5	2.839	2.3	0.1256	4.0	6.103	4.6	0.3523	2.3	0.49
1_14.1	0.13	283	72.8	87.5	0.27	1983	27	2036	22	3	2.777	1.6	0.1255	1.2	6.233	2.0	0.3601	1.6	0.79
1_5.1	1.42	98.6	131	32.0	1.37	2041	37	1966	82	-4	2.686	2.1	0.1206	4.6	6.194	5.1	0.3724	2.1	0.41
1_24.1	1.00	522	81.6	173	0.16	2087	29	2602	21	25	2.615	1.7	0.1746	1.3	9.203	2.1	0.3824	1.7	0.80
1_7.1	0.81	223	125	74.2	0.58	2095	30	2045	41	-2	2.605	1.7	0.1261	2.3	6.678	2.9	0.3839	1.7	0.58
1_18.1	0.23	651	122	215	0.19	2096	27	2086	15	0	2.602	1.5	0.1291	0.9	6.840	1.8	0.3843	1.5	0.87
2_5.1	0.63	2444	117	944	0.05	2380	20	2564	8.8	8	2.239	1.0	0.1706	0.5	10.51	1.1	0.4466	1.0	0.88
1_23.2	0.24	1204	8.64	477	0.01	2392	20	2568	11	7	2.225	1.0	0.1710	0.6	10.60	1.2	0.4493	1.0	0.85
2_23.2	0.09	897	8.34	352	0.01	2420	21	2563	11	6	2.195	1.0	0.1705	0.6	10.71	1.2	0.4557	1.0	0.85
1_23.2	0.03	1211	15.2	466	0.01	2433	20	2575	13	6	2.181	1.0	0.1717	0.8	10.86	1.3	0.4586	1.0	0.78
1_21.2	0.02	1383	41.0	558	0.03	2484	21	2565	9.4	3	2.127	1.0	0.1707	0.6	11.07	1.2	0.4701	1.0	0.87
2_14.1	0.25	1216	12.8	495	0.01	2496	22	2586	12	4	2.115	1.1	0.1729	0.7	11.27	1.3	0.4728	1.1	0.82
1_24.2	0.07	1770	62.8	720	0.04	2496	20	2569	8.7	3	2.115	1.0	0.1711	0.5	11.16	1.1	0.4728	1.0	0.88
2_23.1	0.05	328	133	134	0.42	2506	24	2668	14	6	2.104	1.1	0.1816	0.8	11.90	1.4	0.4752	1.1	0.81
1_19.2	0.04	1645	46.7	673	0.03	2509	20	2590	8.7	3	2.101	1.0	0.1733	0.5	11.37	1.1	0.4759	1.0	0.88
2_11.1	0.07	987	10.2	408	0.01	2532	21	2576	8.8	2	2.078	1.0	0.1719	0.5	11.40	1.1	0.4811	1.0	0.88
2_8.1	0.08	1792	44.4	742	0.03	2533	21	2581	8.1	2	2.078	1.0	0.1724	0.5	11.44	1.1	0.4813	1.0	0.90
1_28.1	0.00	132	413	55.2	3.22	2550	43	2696	24	6	2.061	2.1	0.1848	1.4	12.36	2.5	0.4852	2.1	0.82
1_29.1	0.67	221	89.7	93.5	0.42	2564	39	2670	23	4	2.047	1.8	0.1819	1.4	12.25	2.3	0.4884	1.8	0.79
1_23.1	0.59	297	156	126	0.54	2574	37	2651	20	3	2.038	1.7	0.1798	1.2	12.16	2.1	0.4907	1.7	0.82
2_9.1	0.29	797	456	338	0.59	2582	22	2676	10	4	2.030	1.0	0.1826	0.6	12.40	1.2	0.4925	1.0	0.87
2_13.1	0.01	919	9.27	390	0.01	2589	27	2601	19	0	2.023	1.3	0.1745	1.1	11.89	1.7	0.4942	1.3	0.75
1_27.1	0.30	540	19.6	230	0.04	2595	35	2592	16	0	2.018	1.6	0.1736	0.9	11.86	1.9	0.4956	1.6	0.87
2_16.2	0.00	285	143	122	0.52	2608	24	2657	12	2	2.005	1.1	0.1805	0.7	12.41	1.3	0.4987	1.1	0.85
1_23.3	0.66	119	38.9	51.5	0.34	2609	32	2663	27	2	2.005	1.5	0.1811	1.6	12.45	2.2	0.4988	1.5	0.68
2_10.1	0.19	1873	65.5	809	0.04	2622	21	2583	7.9	-1	1.993	1.0	0.1726	0.5	11.95	1.1	0.5019	1.0	0.90
2_16.1	0.64	970	60.6	421	0.06	2626	21	2604	10	-1	1.989	1.0	0.1748	0.6	12.12	1.2	0.5028	1.0	0.85
2_12.1	0.07	1942	60.1	840	0.03	2627	25	2595	15	-1	1.988	1.1	0.1739	0.9	12.06	1.5	0.5031	1.1	0.78
2_19.1	0.14	325	121	141	0.38	2627	24	2664	12	1	1.987	1.1	0.1812	0.7	12.57	1.3	0.5032	1.1	0.85
2_4.1	0.04	867	252	377	0.30	2638	22	2663	8.7	1	1.977	1.0	0.1811	0.5	12.63	1.1	0.5058	1.0	0.88
2_17.1	0.14	757	386	330	0.53	2642	21	2673	8.8	1	1.974	1.0	0.1822	0.5	12.73	1.1	0.5066	1.0	0.88
1_21.1	0.63	149	69.0	65.7	0.48	2652	43	2682	30	1	1.965	2.0	0.1832	1.8	12.85	2.7	0.5089	2.0	0.74
2_1.1	0.11	520	307	229	0.61	2660	22	2681	8.8	1	1.958	1.0	0.1830	0.5	12.89	1.1	0.5108	1.0	0.89
1_11.1	0.09	292	89.5	129	0.32	2673	34	2651	17	-1	1.946	1.5	0.1798	1.0	12.74	1.9	0.5138	1.5	0.83
2_14.2	0.00	127	52.0	56.1	0.42	2676	37	2689	28	0	1.944	1.7	0.1839	1.7	13.05	2.4	0.5145	1.7	0.71
2_18.1	0.46	144	48.6	64.0	0.35	2678	29	2695	21	1	1.941	1.3	0.1846	1.3	13.11	1.8	0.5151	1.3	0.72
2_20.1	0.05	618	369	276	0.62	2694	22	2681	10	0	1.927	1.0	0.1831	0.6	13.10	1.2	0.5189	1.0	0.87
2_3.1	0.03	696	168	311	0.25	2697	22	2666	7.8	-1	1.925	1.0	0.1815	0.5	13.00	1.1	0.5196	1.0	0.90
1_20.1	0.71	171	88.2	76.9	0.53	2699	42	2665	27	-1	1.923	1.9	0.1814	1.6	13.01	2.5	0.5200	1.9	0.76
2_24.1	0.35	185	79.2	83.0	0.44	2706	28	2653	20	-2	1.917	1.3	0.1801	1.2	12.95	1.8	0.5216	1.3	0.72
1_22.1	0.09	756	278	340	0.38	2712	34	2686	12	-1	1.912	1.6	0.1836	0.7	13.24	1.7	0.5229	1.6	0.91
1_25.1	0.46	195	88.8	88.0	0.47	2716	41	2674	22	-2	1.908	1.9	0.1823	1.3	13.17	2.3	0.5240	1.9	0.82
2_7.1	0.12	584	65.2	265	0.12	2736	23	2688	9.3	-2	1.891	1.0	0.1839	0.6	13.41	1.2	0.5288	1.0	0.88
1_19.1	0.05	1329	202	605	0.16	2741	33	2693	10	-2	1.887	1.5	0.1845	0.6	13.48	1.6	0.5300	1.5	0.92
2_22.1	0.06	612	226	279	0.38	2747	25	2688	13	-2	1.882	1.1	0.1839	0.8	13.47	1.4	0.5313	1.1	0.81
2_21.1	0.03	328	127	150	0.40	2747	24	2691	11	-2	1.882	1.1	0.1842	0.7	13.50	1.3	0.5314	1.1	0.85
2_13.2	0.06	1000	743	459	0.77	2756	22	2671	10	-3	1.874	1.0	0.1820	0.6	13.39	1.2	0.5335	1.0	0.86
2_15.1	0.02	1765	615	818	0.36	2781	21	2674	5.8	-4	1.854	0.9	0.1823	0.3	13.56	1.0	0.5393	0.9	0.94
2_2.1	0.03	2173	481	1011	0.23	2791	21	2673	6.1	-4	1.846	0.9	0.1822	0.4	13.61	1.0	0.5417	0.9	0.93
2_7.2	0.05	925	690	438	0.77	2831	23	2679	8.4	-5	1.813	1.0	0.1828	0.5	13.90	1.1	0.5514	1.0	0.89

Table 1. Continued.

Analysis number	% $^{206}Pb_c$	ppm U	ppm Th	ppm $^{206}Pb^*$	$^{232}Th/^{238}U$	(1) $^{206}Pb/^{238}U$ Age (Ma) ± abs		(1) $^{207}Pb/^{206}Pb$ Age (Ma) ± abs		% Dis.	(1) $^{238}U/^{206}Pb^*$	±%	(1) $^{207}Pb^*/^{206}Pb^*$	±%	(1) $^{207}Pb^*/^{235}U$	±%	(1) $^{206}Pb^*/^{238}U$	±%	err corr
2_6.1	0.02	1176	678	558	0.60	2836	22	2680	7.8	-5	1.809	1.0	0.1830	0.5	13.95	1.1	0.5527	1.0	0.90
Granitoid fragments from the Mendeleev Rise, sample AF05-24 (79°N, 178°W)																			
2.1	4.38	861	402	184	0.48	1353	16	2604	20	92	4.214	1.3	0.1748	1.2	5.630	1.8	0.2335	1.3	0.73
13.1	3.52	2869	353	714	0.13	1576	7.7	2233	26	42	3.575	0.6	0.1405	1.5	5.362	1.6	0.2769	0.6	0.34
4.1	0.60	949	240	228	0.26	1580	9.0	2603	9.5	65	3.593	0.7	0.1746	0.6	6.687	0.9	0.2777	0.7	0.75
1_1.1	0.89	1450	305	356	0.22	1607	9.0	2246	17	40	3.534	0.6	0.1415	1.0	5.524	1.2	0.2830	0.6	0.55
1_2.1	4.79	2834	856	795	0.31	1731	20	2512	82	45	3.247	1.3	0.1649	4.9	7.030	5.0	0.3080	1.3	0.26
1_1.2	1.61	980	386	272	0.41	1774	21	2267	17	28	3.157	1.3	0.1432	1.0	6.260	1.7	0.3168	1.3	0.81
10.1	0.00	3051	222	876	0.08	1859	8.8	2270	5.1	22	2.992	0.5	0.1435	0.3	6.613	0.6	0.3342	0.5	0.88
1.1	0.78	687	457	205	0.69	1909	9.6	2617	10	37	2.894	0.6	0.1761	0.6	8.367	0.8	0.3446	0.6	0.69
11.1	1.56	1818	170	582	0.10	2007	9.7	2289	13	14	2.725	0.6	0.1451	0.8	7.307	0.9	0.3653	0.6	0.60
3.1	2.21	492	174	165	0.37	2071	59	2636	24	27	2.618	3.3	0.1782	1.4	9.310	3.6	0.3790	3.3	0.92
8.1	0.90	703	302	241	0.44	2145	15	2609	9.5	22	2.524	0.8	0.1753	0.6	9.546	1.0	0.3949	0.8	0.83
5.1	1.66	499	300	174	0.62	2159	16	2627	19	22	2.499	0.9	0.1772	1.1	9.720	1.4	0.3978	0.9	0.61
7.1	0.29	565	472	209	0.86	2301	12	2630	7.9	14	2.328	0.6	0.1775	0.5	10.50	0.8	0.4290	0.6	0.79
6.1	1.33	303	105	121	0.36	2423	14	2624	14	8	2.181	0.7	0.1770	0.9	11.13	1.1	0.4563	0.7	0.62
9.1	0.00	479	115	196	0.25	2512	13	2613	7.3	4	2.098	0.6	0.1758	0.4	11.55	0.8	0.4766	0.6	0.82
12.1	0.26	1042	526	442	0.52	2578	13	2610	14	1	2.032	0.6	0.1754	0.9	11.89	1.0	0.4918	0.6	0.59
Granitoid fragments from the Mendeleev Rise, sample AF05-26 (79°N, 178°W)																			
3.1	0.00	466	375	96.6	0.83	1393	13	2599	22	86	4.144	1.0	0.1742	1.3	5.796	1.6	0.2413	1.0	0.61
1.1	0.64	716	435	151	0.63	1407	12	2325	18	65	4.099	1.0	0.1482	1.0	4.984	1.4	0.2440	1.0	0.68
7.1	1.52	389	405	96.1	1.07	1607	16	2331	28	45	3.533	1.1	0.1487	1.6	5.800	2.0	0.2831	1.1	0.58
5.1	2.26	1147	349	328	0.31	1817	15	2330	18	28	3.072	1.0	0.1486	1.0	6.669	1.4	0.3255	1.0	0.68
10.1	0.46	754	606	222	0.83	1890	16	2339	13	24	2.936	1.0	0.1494	0.7	7.017	1.2	0.3406	1.0	0.80
4.1	0.00	1107	832	340	0.78	1971	16	2602	8.2	32	2.795	1.0	0.1746	0.5	8.610	1.1	0.3577	1.0	0.89
12.1	0.76	577	304	192	0.54	2098	18	2321	27	11	2.600	1.0	0.1479	1.6	7.840	1.8	0.3846	1.0	0.54
8.1	1.93	561	206	192	0.38	2123	18	2353	24	11	2.564	1.0	0.1506	1.4	8.100	1.7	0.3901	1.0	0.57
2.1	0.13	428	545	149	1.32	2194	19	2615	11	19	2.467	1.0	0.1760	0.7	9.840	1.2	0.4054	1.0	0.83
2.2	0.00	423	402	150	0.98	2228	20	2625	10	18	2.422	1.0	0.1770	0.6	10.08	1.2	0.4129	1.0	0.86
6.1	0.00	533	161	198	0.31	2313	19	2624	9.4	13	2.317	10	0.1769	0.6	10.53	1.1	0.4316	10	0.87
9.1	0.00	352	296	147	0.87	2557	22	2622	11	3	2.054	1.0	0.1767	0.7	11.86	1.2	0.4870	1.0	0.84
11.1	0.17	1079	1451	497	1.39	2762	23	2323	9.4	-16	1.869	1.0	0.1480	0.6	10.92	1.2	0.5350	1.0	0.88
Granitoid fragment from the Mendeleev Rise, sample BC-260 (80°N, 179°30'W)																			
4.1r	2.40	12073	4824	189	0.41	114	6.4	1744	38	1434	56.20	5.7	0.1067	2.1	0.262	6.1	0.0178	5.7	0.94
4.1	2.66	9257	4296	224	0.48	174	1.6	1822	47	947	36.55	0.9	0.1113	2.6	0.420	2.8	0.0274	0.9	0.33
7_3.1	3.12	3431	4078	144	1.23	299	6.3	1705	71	471	21.08	2.1	0.1044	3.8	0.683	4.4	0.0474	2.1	0.49
5.1	1.33	5145	5481	226	1.10	317	2.6	1805	51	469	19.82	0.9	0.1103	2.8	0.767	2.9	0.0504	0.9	0.29
4_2.1	1.30	4308	1904	236	0.46	393	4.7	1850	24	371	15.91	1.2	0.1131	1.3	0.980	1.8	0.0628	1.2	0.69
3.1	1.21	4915	686	280	0.14	410	3.3	1922	23	369	15.24	0.8	0.1177	1.3	1.065	1.5	0.0656	0.8	0.54
6.1	2.35	3530	1132	230	0.33	461	6.3	1892	97	311	13.48	1.4	0.1157	5.4	1.183	5.6	0.0741	1.4	0.25
1.2	1.86	2573	273	289	0.11	777	21	1931	37	148	7.790	2.9	0.1183	2.1	2.091	3.6	0.1282	2.9	0.81
7_2.1	1.16	3043	6097	348	2.07	796	7.9	1968	30	147	7.599	1.0	0.1208	1.7	2.190	2.0	0.1315	1.0	0.53
1.1	0.21	2077	49.7	359	0.02	1178	7.1	1933	30	64	4.985	0.7	0.1184	1.7	3.275	1.8	0.2006	0.7	0.36
7.1	1.42	1392	270	245	0.20	1183	18	1971	35	67	4.957	1.7	0.1210	2.0	3.361	2.6	0.2014	1.7	0.64
Metagabbro-dolerite fragments from the Mendeleev Rise, sample AF05-11 (78°55'N, 177°40'W)																			
31_1.1	0.70	168	67.1	17.9	0.41	750	9.4	818	102	9	8.101	1.3	0.0664	4.9	1.130	5.1	0.1234	1.3	0.26
31_1.2	0.00	253	145	28.8	0.59	801	8.7	811	37	1	7.561	1.2	0.0661	1.8	1.206	2.1	0.1323	1.2	0.54
31_2.1	9.57	412	841	83.2	2.11	1242	14	1904	85	53	4.705	1.3	0.1166	4.7	3.415	4.9	0.2125	1.3	0.26
31_3.1	16.3	486	1152	107	2.45	1248	16	1989	98	59	4.682	1.4	0.1222	5.5	3.599	5.7	0.2136	1.4	0.24
31_3.2	10.4	442	748	149	1.75	1946	27	1958	94	1	2.838	1.6	0.1201	5.3	5.836	5.5	0.3524	1.6	0.29
31_4.1	7.73	1485	1476	370	1.03	1528	15	1923	43	26	3.738	1.1	0.1178	2.4	4.344	2.6	0.2675	1.1	0.43
31_5.1	0.00	95.2	16.0	28.7	0.17	1940	24	1962	30	1	2.848	1.4	0.1204	1.7	5.828	2.2	0.3511	1.4	0.65
31_6.1	0.13	709	224	317	0.33	2700	22	2661	8	-1	1.923	1.0	0.1809	0.5	12.97	1.1	0.5201	1.0	0.90
31_6.2	1.33	1905	102	815	0.06	2577	20	2652	9	3	2.034	1.0	0.1799	0.5	12.19	1.1	0.4915	1.0	0.88
31_7.1	0.15	440	130	197	0.31	2701	22	2673	10	-1	1.921	1.0	0.1822	0.6	13.08	1.2	0.5205	1.0	0.86
32_1.1	0.09	1895	2294	193	1.25	nd	nd	776	20	nd	nd	nd	0.0651	0.9	nd	nd	nd	nd	nd
Metagabbro-dolerite fragments from the Mendeleev Rise (measurements in thin sections), sample AF05-26 (79°N, 178°W)																			
1.1	0.46	6991	24825	445	3.67	nd		720	15	nd	nd	nd	0.0633	0.7	nd	nd	nd	nd	nd
2.1	0.55	1067	557	99.8	0.54	nd	nd	828	30	nd	nd	nd	0.0667	1.4	nd	nd	nd	nd	nd
2.2	0.48	2090	2055	207	1.02	nd	nd	786	21	nd	nd	nd	0.0654	1.0	nd	nd	nd	nd	nd
3.1	0.48	1499	1076	147	0.74	nd	nd	800	28	nd	nd	nd	0.0658	1.3	nd	nd	nd	nd	nd
3.2	0.43	1063	611	105	0.59	nd	nd	816	56	nd	nd	nd	0.0663	2.7	nd	nd	nd	nd	nd
4.1	0.67	1006	263	109	0.27	nd	nd	804	33	nd	nd	nd	0.0659	1.6	nd	nd	nd	nd	nd
5.1	1.14	12374	36736	806	3.07	nd	nd	717	48	nd	nd	nd	0.0633	2.3	nd	nd	nd	nd	nd
6.1	3.52	1729	1117	198	0.67	nd	nd	836	268	nd	nd	nd	0.0669	13	nd	nd	nd	nd	nd
7.1	3.96	2938	3131	240	1.10	nd	nd	733	123	nd	nd	nd	0.0638	5.8	nd	nd	nd	nd	nd
7.2	0.86	2884	4809	221	1.72	nd	nd	723	29	nd	nd	nd	0.0634	1.4	nd	nd	nd	nd	nd
8.1	0.89	1559	937	173	0.62	nd	nd	859	60	nd	nd	nd	0.0677	2.9	nd	nd	nd	nd	nd
9.1	1.80	3550	8734	220	2.54	nd	nd	760	39	nd	nd	nd	0.0646	1.8	nd	nd	nd	nd	nd
10.1	11.1	934	1467	132	1.62	nd	nd	839	210	nd	nd	nd	0.0670	10	nd	nd	nd	nd	nd
11.1	13.4	964	1532	117	1.64	nd	nd	397	610	nd	nd	nd	0.0546	27	nd	nd	nd	nd	nd
Sandstone fragments from the Mendeleev Rise, samples AF00-05 (1, 2) (82°10 N, 178°W)																			
2_6.1	1.20	3429	1583	104	0.48	221	0.8	1561	24	606	28.68	0.3	0.0967	1.3	0.465	1.3	0.0349	0.3	0.26
1_8.1	---	887	496	29.4	0.58	243	1.8	119	53	-51	25.91	0.8	0.0507	1.9	0.270	2.0	0.0386	0.8	0.37
1_9.1	0.32	252	119	9.86	0.49	284	4.6	-82	206	-129	22.04	1.7	0.0515	3.7	0.322	4.1	0.0454	1.7	0.40
1_2.1	0.01	833	388	32.5	0.48	286	2.1	201	71	-30	21.99	0.7	0.0522	1.8	0.327	1.9	0.0455	0.7	0.38
1_10.1	0.34	264	188	10.6	0.74	291	3.2	-8	193	-103	21.47	1.1	0.0521	3.7	0.335	3.8	0.0466	1.1	0.29
2_6.2	0.38	2056	1036	88.2	0.52	313	1.0	1675	13	435	20.10	0.3	0.1028	0.7	0.705	0.8	0.0498	0.3	0.42
1_4.1	0.42	110	72.1	5.02	0.68	327	5.3	-451	611	-238	18.89	1.6	0.0520	5.7	0.379	6.0	0.0529	1.6	0.28
2_18.1	0.23	421	160	24.5	0.39	421	3.0	446	66	6	14.82	0.7	0.0558	3.0	0.520	3.1	0.0675	0.7	0.24
2_17.1	0.65	16.6	0.166	0.97	0.01	422	11	178	478	-58	14.78	2.7	0.0496	20	0.463	21	0.0677	2.7	0.13
2_25.1	0.46	419	93.6	25.8	0.23	444	3.0	450	86	1	14.04	0.7	0.0559	3.9	0.549	3.9	0.0712	0.7	0.18
2_16.1	0.22	126	87.9	7.98	0.72	456	4.3	234	74	-49	13.63	1.0	0.0509	3.2	0.514	3.4	0.0734	1.0	0.29
1_1.1	0.11	172	126	15.7	0.76	648	7.0	523	119	-19	9.404	1.1	0.0622	3.4	0.912	3.6	0.1063	1.1	0.32
2_23.1	0.20	89	42.0	9.21	0.49	734	7.9	770	73	5	8.291	1.1	0.0649	3.5	1.079	3.7	0.1206	1.1	0.31
2_4.1	0.00	622	57.8	81.7	0.10	917	3.7	882	33	-4	6.540	0.4	0.0684	1.6	1.443	1.7	0.1529	0.4	0.26
2_12.1	0.11	156	97.2	20.7	0.65	927	6.7	912	35	-2	6.464	0.8	0.0694	1.7	1.481	1.8	0.1547	0.8	0.42
2_9.1	0.25	235	80.5	32.9	0.35	971	5.1	888	36	-9	6.150	0.6	0.0686	1.8	1.539	1.8	0.1626	0.6	0.31
2_28.1	0.08	709	270	101	0.39	991	4.3	1032	21	4	6.018	0.5	0.0737	1.0	1.688	1.1	0.1662	0.5	0.40
2_19.1	---	323	96.8	47.4	0.31	1016	5.2	1038	25	2	5.857	0.6	0.0739	1.3	1.739	1.4	0.1707	0.6	0.40
2_30.1	0.05	370	79.3	57.4	0.22	1069	5.1	1072	24	0	5.544	0.5	0.0751	1.2	1.868	1.3	0.1804	0.5	0.40
2_22.1	0.19	121	54.8	20.3	0.47	1145	9.3	1182	52	3	5.143	0.9	0.0794	2.6	2.128	2.8	0.1944	0.9	0.32
2_15.1	0.03	385	172	64.6	0.46	1150	5.0	1157	15	1	5.119	0.5	0.0784	0.7	2.111	0.9	0.1953	0.5	0.54
2_11.1	0.03	345	244	58.6	0.73	1162	4.6	1157	15	0	5.061	0.4	0.0784	0.8	2.135	0.9	0.1976	0.4	0.49

Table 1. Continued.

Analysis number	% $^{206}Pb_c$	ppm U	ppm Th	ppm $^{206}Pb*$	$^{232}Th/^{238}U$	(1) $^{206}Pb/^{238}U$ Age (Ma)	± abs	(1) $^{207}Pb/^{206}Pb$ Age (Ma)	± abs	% Dis.	(1) $^{238}U/^{206}Pb^*$	±%	(1) $^{207}Pb^{*}/^{206}Pb^*$	±%	(1) $^{207}Pb^{*}/^{235}U$	±%	(1) $^{206}Pb^{*}/^{238}U$	±%	err corr
2_10.1	0.03	155	55.6	28.3	0.37	1239	7.5	1135	23	-8	4.718	0.7	0.0775	1.1	2.266	1.3	0.2120	0.7	0.50
1_6.1	0.12	310	80.9	57.9	0.27	1263	9.1	1707	26	35	4.612	0.8	0.1057	1.3	3.160	1.5	0.2168	0.8	0.53
2_26.1	0.08	164	70.0	33.7	0.44	1381	10	1387	30	0	4.185	0.8	0.0882	1.6	2.906	1.8	0.2390	0.8	0.47
2_14.1	0.06	210	90.0	43.6	0.44	1394	7.8	1360	17	-2	4.142	0.6	0.0870	0.9	2.896	1.1	0.2414	0.6	0.57
2_21.1	0.16	57.0	30.0	12.9	0.54	1504	16	1581	43	5	3.805	1.2	0.0977	2.3	3.541	2.6	0.2628	1.2	0.45
1_3.1	0.19	372	510	96.2	1.41	1691	11	1839	17	9	3.330	0.7	0.1130	0.8	4.681	1.1	0.3003	0.7	0.66
2_3.1	0.02	365	224	95.6	0.63	1714	9.4	1849	13	8	3.282	0.6	0.1131	0.7	4.749	1.0	0.3047	0.6	0.66
2_13.1	0.05	92.7	44.2	24.7	0.49	1741	14	1744	19	0	3.226	0.9	0.1067	1.0	4.562	1.4	0.3100	0.9	0.65
2_29.1	0.17	107	41.8	29.3	0.40	1778	13	1918	27	8	3.148	0.8	0.1174	1.5	5.144	1.7	0.3177	0.8	0.48
1_5.1	---	27.7	15.0	7.68	0.56	1795	36	1648	81	-8	3.080	2.3	0.1100	3.9	4.924	4.6	0.3247	2.3	0.50
2_24.1	0.02	136	35.0	37.9	0.27	1808	12	1822	22	1	3.089	0.7	0.1114	1.2	4.970	1.4	0.3237	0.7	0.52
2_2.1	0.03	315	126	91.8	0.42	1885	8.9	1997	11	6	2.944	0.5	0.1228	0.6	5.750	0.8	0.3396	0.5	0.66
2_1.1	0.12	78.5	62.8	23.3	0.83	1912	17	1842	27	-4	2.896	1.0	0.1126	1.5	5.361	1.8	0.3453	1.0	0.57
2_20.1	---	335	150	101	0.46	1938	9.0	1933	13	0	2.851	0.5	0.1184	0.8	5.727	0.9	0.3508	0.5	0.58
2_5.1	0.01	255	162	77.4	0.66	1951	11	1997	11	2	2.830	0.7	0.1228	0.6	5.982	0.9	0.3534	0.7	0.72
1_7.1	0.19	207	136	63.8	0.68	1975	15	1979	19	0	2.785	0.9	0.1225	1.0	6.067	1.3	0.3591	0.9	0.67
2_8.1	0.01	115	76.0	35.5	0.68	1976	12	1991	14	1	2.788	0.7	0.1224	0.8	6.051	1.0	0.3587	0.7	0.67
2_17.2	0.14	75.5	55.6	23.5	0.76	1989	15	1993	19	0	2.767	0.9	0.1225	1.1	6.103	1.4	0.3613	0.9	0.63
2_27.1	0.06	151	78.1	62.1	0.53	2514	14	2560	14	2	2.097	0.7	0.1703	0.8	11.20	1.1	0.4770	0.7	0.62
2_7.1	0.02	527	345	226	0.68	2611	8.0	2716	4.4	4	2.003	0.4	0.1870	0.3	12.87	0.5	0.4992	0.4	0.82
Sandstone fragments from the Mendeleev Rise, sample AF00-10 (82°04'N, 179°59'W)																			
15.2	1.71	1929	980	64.2	0.53	241	1.0	552	91	129	26.24	0.4	0.0586	4.2	0.308	4.2	0.0381	0.4	0.10
15.1	1.60	1459	693	60.6	0.49	300	1.4	567	68	89	21.02	0.5	0.0590	3.1	0.387	3.1	0.0476	0.5	0.15
26.1	1.00	1008	172	49.0	0.18	352	1.7	393	74	12	17.83	0.5	0.0545	3.3	0.421	3.4	0.0561	0.5	0.15
5.1	0.66	900	963	47.9	1.11	385	2.5	350	70	-9	16.24	0.7	0.0548	2.6	0.454	3.2	0.0615	0.7	0.21
8.1	1.44	1585	737	109	0.48	490	6.3	1465	44	199	12.64	1.3	0.0925	2.2	1.001	2.7	0.0790	1.3	0.50
3.1	---	436	209	34.3	0.49	564	4.9	481	39	-15	10.91	0.9	0.0587	1.8	0.742	2.0	0.0917	0.9	0.45
20.1	1.15	1799	1466	205	0.84	795	4.2	1539	63	94	7.619	0.6	0.0955	3.3	1.729	3.4	0.1313	0.6	0.17
1.1	0.07	774	373	106	0.50	949	5.5	920	25	-3	6.297	0.6	0.0704	1.0	1.525	1.4	0.1587	0.6	0.46
22.1	0.64	826	32.8	115	0.04	965	3.9	1186	27	23	6.193	0.4	0.0796	1.4	1.772	1.5	0.1615	0.4	0.30
25.1	0.23	151	112	21.0	0.77	965	7.4	995	54	3	6.193	0.8	0.0723	2.7	1.610	2.8	0.1615	0.8	0.29
27.1	0.01	316	159	52.1	0.52	1132	7.0	1154	25	2	5.208	0.7	0.0783	1.2	2.073	1.4	0.1920	0.7	0.48
7.1	---	60.8	40.8	10.2	0.69	1147	17	1013	81	-12	5.094	1.6	0.0795	2.7	1.959	4.3	0.1947	1.6	0.37
21.1	1.24	42.6	73.5	10.5	1.78	1612	19	1668	75	3	3.520	1.3	0.1024	4.1	4.010	4.3	0.2841	1.3	0.31
29.1	0.01	293	132	73.4	0.47	1651	7.8	1664	16	1	3.427	0.5	0.1022	0.9	4.110	1.0	0.2918	0.5	0.52
11.1	0.28	44.8	52.5	11.9	1.21	1731	25	1738	46	0	3.246	1.6	0.1064	2.5	4.518	3.0	0.3080	1.6	0.54
30.1	---	66.7	35.7	17.8	0.55	1739	16	1748	32	1	3.229	1.0	0.1069	1.7	4.565	2.0	0.3097	1.0	0.51
28.1	0.05	132	44.3	36.1	0.35	1785	12	1821	22	2	3.135	0.8	0.1113	1.2	4.896	1.4	0.3190	0.8	0.52
16.1	0.10	436	113	121	0.27	1801	6.3	1858	12	3	3.103	0.4	0.1136	0.7	5.048	0.8	0.3223	0.4	0.53
17.1	0.10	157	67.7	44.9	0.45	1854	23	1932	24	4	3.002	1.4	0.1184	1.4	5.438	2.0	0.3331	1.4	0.73
4.1	0.50	272	76.0	78.9	0.29	1862	14	1884	23	1	2.980	0.9	0.1160	1.1	5.322	1.5	0.3349	0.9	0.58
10.1	---	193	86.9	55.5	0.47	1866	15	1841	20	-1	2.976	0.9	0.1137	1.3	5.209	1.4	0.3357	0.9	0.64
24.1	0.09	634	317	183	0.52	1868	5.8	1966	17	5	2.975	0.4	0.1207	0.9	5.593	1.0	0.3361	0.4	0.36
9.2	---	98.9	32.9	29.2	0.34	1900	20	1877	27	-1	2.910	1.2	0.1169	1.4	5.424	1.9	0.3427	1.2	0.62
13.1	0.27	133	59.0	39.6	0.46	1914	15	1982	23	4	2.893	0.9	0.1218	1.3	5.804	1.6	0.3456	0.9	0.58
14.1	0.09	82.8	58.4	24.8	0.73	1927	16	1962	25	2	2.870	1.0	0.1204	1.4	5.784	1.7	0.3484	1.0	0.57
2.1	0.13	311	141	95.0	0.47	1957	13	1957	15	0	2.816	0.8	0.1207	0.8	5.873	1.1	0.3547	0.8	0.67
19.1	0.05	376	348	115	0.96	1958	8.6	1989	12	2	2.817	0.5	0.1222	0.7	5.982	0.9	0.3550	0.5	0.59
12.1	0.35	207	110	63.4	0.55	1962	11	1980	23	1	2.812	0.7	0.1216	1.3	5.962	1.4	0.3557	0.7	0.46
9.1	---	412	59.5	128	0.15	1988	12	1956	12	-2	2.768	0.7	0.1205	0.7	5.974	1.0	0.3612	0.7	0.72
18.1	0.05	381	183	120	0.50	2018	7.3	2014	11	0	2.720	0.4	0.1239	0.6	6.282	0.7	0.3676	0.4	0.58
23.1	0.19	52.9	22.9	17.0	0.45	2042	19	2034	34	0	2.684	1.1	0.1254	1.9	6.440	2.2	0.3726	1.1	0.50
6.1	---	373	163	168	0.45	2722	27	2706	8.0	-1	1.903	1.2	0.1862	0.5	13.47	1.3	0.5254	1.2	0.93
Sandstone fragments from the Mendeleev Rise, sample AF05-11 (78°55'N, 177°40'W)																			
4_20.1	0.00	22.2	19.2	0.83	0.89	274	20	352	446	28	23.01	7.6	0.0535	20	0.321	21	0.0435	7.6	0.360
4_20.2	0.00	27.6	22.5	1.10	0.84	292	16	492	316	69	21.61	5.5	0.0570	14	0.364	15	0.0463	5.5	0.357
6_3.1	0.63	1984	3426	150	1.78	541	3.4	1598	33	195	11.43	0.7	0.0986	1.7	1.189	1.9	0.0875	0.7	0.353
6_5.1	0.74	2091	926	169	0.46	577	3.0	1489	27	158	10.68	0.5	0.0931	1.4	1.201	1.5	0.0936	0.5	0.360
6_19.1	0.69	1563	446	127	0.29	578	3.4	1124	41	95	10.66	0.6	0.0771	2.1	0.997	2.1	0.0938	0.6	0.286
6_9.1	0.74	1056	945	87.3	0.93	588	3.9	1360	52	131	10.46	0.7	0.0870	2.7	1.146	2.8	0.0956	0.7	0.249
6_8.1	0.65	1056	386	96.3	0.38	646	4.1	1100	52	70	9.483	0.7	0.0762	2.6	1.108	2.7	0.1055	0.7	0.249
6_1.1	0.23	1348	968	124	0.74	655	3.3	1224	26	87	9.344	0.5	0.0811	1.3	1.197	1.4	0.1070	0.5	0.364
6_7.1	0.90	478	322	46.0	0.70	679	6.5	1388	78	104	9.002	1.0	0.0883	4.0	1.352	4.2	0.1111	1.0	0.242
6_20.1	0.23	870	178	84.5	0.21	688	4.6	1192	37	73	8.874	0.7	0.0798	1.9	1.240	2.0	0.1127	0.7	0.351
6_15.1	0.84	186	155	26.5	0.86	979	16	1062	154	8	6.097	1.7	0.0748	7.6	1.691	7.8	0.1640	1.7	0.219
4_2.1	1.95	106	35.9	16.2	0.35	1037	21	1032	216	0	5.731	2.2	0.0737	11	1.772	11	0.1745	2.2	0.197
6_21.1	0.28	670	248	102	0.38	1048	6.6	1067	37	2	5.665	0.7	0.0750	1.9	1.824	2.0	0.1765	0.7	0.344
6_18.1	1.00	167	61.1	25.9	0.38	1057	13	1053	139	0	5.611	1.3	0.0744	6.9	1.828	7.0	0.1782	1.3	0.190
6_4.1	1.88	77.7	45.5	12.2	0.61	1063	18	1077	184	1	5.578	1.8	0.0753	9.2	1.861	9.3	0.1793	1.8	0.197
4_17.1	3.91	29.4	22.5	4.89	0.79	1100	32	1242	331	13	5.377	3.2	0.0818	17	2.098	17	0.1860	3.2	0.185
4_21.1	0.41	146	69.4	23.5	0.49	1105	11	1121	67	1	5.346	1.1	0.0770	3.4	1.986	3.5	0.1871	1.1	0.316
6_17.1	0.22	159	83.4	25.6	0.54	1106	14	1170	52	6	5.346	1.4	0.0789	2.6	2.035	2.9	0.1871	1.4	0.467
6_14.1	0.02	159	93.0	25.8	0.60	1114	12	1122	75	1	5.301	1.2	0.0770	3.8	2.004	3.9	0.1886	1.2	0.305
6_25.1	0.75	157	89.1	25.9	0.59	1122	14	1208	103	8	5.260	1.3	0.0804	5.2	2.108	5.4	0.1901	1.3	0.248
4_8.1	3.02	21.7	9.68	3.70	0.46	1138	38	1546	257	36	5.181	3.7	0.0959	14	2.552	14	0.1930	3.7	0.260
6_6.1	0.57	164	118	28.5	0.74	1177	13	1264	87	7	4.991	1.2	0.0828	4.5	2.286	4.6	0.2004	1.2	0.260
6_2.1	0.61	427	133	74.8	0.32	1190	8.7	1220	41	3	4.931	0.8	0.0810	2.1	2.264	2.2	0.2028	0.8	0.357
4_14.1	0.17	303	113	54.7	0.38	1229	10	1257	40	2	4.761	0.9	0.0825	2.1	2.388	2.3	0.2101	0.9	0.411
4_6.1	0.18	185	63.9	34.8	0.36	1274	13	1333	46	5	4.578	1.1	0.0858	2.4	2.583	2.6	0.2184	1.1	0.439
4_10.1	5.62	25.7	27.7	5.17	1.11	1288	48	1375	499	7	4.522	4.1	0.0876	26	2.672	26	0.2211	4.1	0.158
6_13.1	0.00	130	52.4	25.1	0.42	1302	15	1356	45	4	4.469	1.2	0.0868	2.3	2.677	2.6	0.2237	1.2	0.473
6_16.1	2.16	29.9	12.8	5.92	0.44	1311	36	1380	298	5	4.436	3.1	0.0879	16	2.732	16	0.2254	3.1	0.193
6_11.1	0.66	31.2	18.3	6.23	0.60	1337	30	1466	136	10	4.338	2.5	0.0919	7.2	2.922	7.6	0.2305	2.5	0.325
4_3.1	0.69	48.2	22.7	10.0	0.49	1387	33	1597	156	15	4.167	2.6	0.0985	8.4	3.261	8.8	0.2400	2.6	0.299
4_4.1	1.32	45.6	18.7	9.68	0.42	1406	34	1470	223	5	4.103	2.7	0.0922	12	3.097	12	0.2437	2.7	0.226
6_23.1	0.96	95.8	42.3	20.3	0.46	1411	21	1414	93	0	4.086	1.7	0.0895	4.9	3.019	5.1	0.2447	1.7	0.325
4_1.1	0.92	39.9	33.0	8.52	0.85	1418	32	1580	115	11	4.063	2.5	0.0976	6.2	3.313	6.7	0.2461	2.5	0.378
4_15.1	0.41	178	77.5	37.7	0.45	1419	14	1422	48	0	4.060	1.1	0.0898	2.5	3.051	2.7	0.2463	1.1	0.390
4_16.1	0.00	134	48.6	28.5	0.38	1427	16	1463	44	3	4.037	1.2	0.0918	2.3	3.135	2.6	0.2477	1.2	0.471
4_7.1	0.38	92.9	55.5	20.0	0.62	1436	20	1448	60	1	4.007	1.6	0.0911	3.2	3.133	3.5	0.2495	1.6	0.446
4_13.1	0.00	198	87.3	42.5	0.46	1438	14	1441	38	0	4.002	1.1	0.0907	2.0	3.126	2.3	0.2499	1.1	0.477
6_12.1	0.14	138	69.2	30.1	0.52	1455	16	1449	48	0	3.948	1.2	0.0911	2.5	3.182	2.8	0.2533	1.2	0.439
4_9.1	1.04	112	94.8	24.6	0.88	1461	19	1609	73	10	3.932	1.4	0.0992	3.9	3.479	4.2	0.2543	1.4	0.344
4_12.1	0.63	93.1	101	20.9	1.12	1489	21	1599	78	7	3.848	1.6	0.0986	4.2	3.535	4.5	0.2599	1.6	0.352

Table 1. Continued.

Analysis number	% $^{206}Pb_c$	ppm U	ppm Th	ppm $^{206}Pb^*$	$^{232}Th/^{238}U$	(1) $^{206}Pb/^{238}U$ Age (Ma)	± abs	(1) $^{207}Pb/^{206}Pb$ Age (Ma)	± abs	% Dis.	(1) $^{238}U/^{206}Pb^*$	±%	(1) $^{207}Pb^*/^{206}Pb^*$	±%	(1) $^{207}Pb^*/^{235}U$	±%	(1) $^{206}Pb^*/^{238}U$	±%	err corr
4_11.1	1.10	19.7	7.62	4.45	0.40	1489	43	1839	161	24	3.848	3.3	0.1124	8.9	4.030	9.5	0.2599	3.3	0.344
4_5.1	1.05	86.0	51.4	19.7	0.62	1509	23	1594	107	6	3.791	1.7	0.0984	5.8	3.579	6.0	0.2638	1.7	0.286
4_19.1	0.10	250	221	61.9	0.92	1632	13	1644	30	1	3.471	0.9	0.1011	1.6	4.016	1.8	0.2881	0.9	0.478
6_10.1	0.26	146	244	37.3	1.72	1668	19	1730	78	4	3.386	1.3	0.1059	4.3	4.312	4.4	0.2954	1.3	0.285
6_26.1	0.11	436	156	128	0.37	1895	11	1849	24	-2	2.926	0.7	0.1130	1.3	5.328	1.5	0.3418	0.7	0.460
6_22.1	0.06	201	162	86.2	0.83	2605	22	2624	16	1	2.008	1.0	0.1769	0.9	12.15	1.4	0.4980	1.0	0.731
4_18.1	0.26	213	155	95.4	0.75	2697	19	2707	17	0	1.925	0.8	0.1860	1.0	13.32	1.3	0.5195	0.8	0.630
6_24.1	0.31	96.6	37.4	44.3	0.40	2751	27	2724	25	-1	1.878	1.2	0.1879	1.5	13.79	1.9	0.5324	1.2	0.619
Sandstone fragments from the Mendeleev Rise, sample AF05-14 (79°N, 172°W)																			
4_4.1	7.30	678	166	40.3	0.25	400	4.1	548	210	37	15.60	1.1	0.0585	9.5	0.516	9.5	0.0639	1.1	0.11
4_2.1	0.09	723	314	40.6	0.45	408	2.8	409	31	0	15.30	0.7	0.0549	1.4	0.495	1.5	0.0653	0.7	0.46
2_23.1	0.00	357	338	22.1	0.98	449	4.2	389	44	-13	13.88	1.0	0.0544	2.0	0.541	2.2	0.0721	1.0	0.44
2_9.1	0.06	779	456	49.2	0.60	457	3.6	432	37	-6	13.61	0.8	0.0555	1.7	0.562	1.9	0.0735	0.8	0.44
4_3.1	0.34	578	182	39.0	0.33	486	3.5	519	47	7	12.77	0.7	0.0577	2.2	0.623	2.3	0.0783	0.7	0.33
4_6.1	0.08	517	243	45.7	0.49	630	4.4	620	26	-2	9.734	0.7	0.0605	1.2	0.856	1.4	0.1027	0.7	0.51
2_5.1	0.00	295	56.3	26.7	0.20	644	7.0	621	48	-4	9.520	1.1	0.0605	2.2	0.877	2.5	0.1051	1.1	0.46
2_26.1	0.12	1372	1700	132	1.28	682	6.0	1175	20	72	8.960	0.9	0.0791	1.0	1.217	1.4	0.1116	0.9	0.67
2_12.1	2.37	707	71.0	81.4	0.10	791	7.4	1423	55	80	7.649	1.0	0.0898	2.9	1.617	3.0	0.1305	1.0	0.33
2_18.1	0.25	130	42.8	19.9	0.34	1055	11	1020	50	-3	5.624	1.1	0.0732	2.4	1.795	2.7	0.1778	1.1	0.41
2_21.1	0.05	567	336	87.2	0.61	1061	7.9	1084	20	2	5.590	0.8	0.0756	1.0	1.864	1.3	0.1789	0.8	0.63
2_16.1	0.00	21.0	5.06	3.45	0.25	1129	21	1115	70	-1	5.220	2.0	0.0768	3.5	2.026	4.1	0.1914	2.0	0.50
2_24.1	0.01	510	211	88.4	0.43	1185	10	1167	18	-2	4.956	1.0	0.0788	0.9	2.192	1.3	0.2018	1.0	0.73
2_15.1	0.00	353	112	61.5	0.33	1191	9.3	1185	22	-1	4.926	0.9	0.0795	1.1	2.225	1.4	0.2030	0.9	0.62
2_31.1	0.09	362	100	64.3	0.29	1211	9.6	1205	22	0	4.840	0.9	0.0803	1.1	2.288	1.4	0.2066	0.9	0.61
4_5.1	0.24	663	248	130	0.39	1321	8.5	1391	16	5	4.396	0.7	0.0884	0.9	2.772	1.1	0.2274	0.7	0.64
2_22.1	0.00	123	34.5	26.2	0.29	1422	14	1400	29	-2	4.053	1.1	0.0888	1.5	3.021	1.9	0.2467	1.1	0.59
4_1.1	0.00	102	68.7	22.8	0.69	1486	12	1471	23	-1	3.856	0.9	0.0922	1.2	3.296	1.5	0.2593	0.9	0.60
2_1.1	0.00	341	96.9	79.5	0.29	1548	12	1541	17	0	3.684	0.9	0.0957	0.9	3.581	1.2	0.2715	0.9	0.70
2_19.1	0.11	162	124	39.2	0.79	1594	14	1606	25	1	3.563	1.0	0.0990	1.3	3.831	1.6	0.2806	1.0	0.60
2_6.1	0.15	233	142	56.9	0.63	1612	15	2739	13	70	3.520	1.0	0.1896	0.8	7.428	1.3	0.2840	1.0	0.78
2_14.1	0.01	388	105	97.1	0.28	1648	12	1635	14	-1	3.434	0.8	0.1006	0.7	4.039	1.1	0.2912	0.8	0.74
2_10.1	0.00	248	167	63.0	0.70	1671	14	1663	20	-1	3.379	0.9	0.1021	1.1	4.167	1.4	0.2959	0.9	0.65
2_7.1	0.00	235	120	60.9	0.53	1698	13	1682	17	-1	3.319	0.9	0.1032	0.9	4.287	1.3	0.3013	0.9	0.70
2_30.1	0.03	291	89.1	77.8	0.32	1747	13	1729	15	-1	3.212	0.9	0.1058	0.8	4.543	1.2	0.3113	0.9	0.73
2_13.1	0.10	211	87.8	58.5	0.43	1804	14	1819	18	1	3.096	0.9	0.1112	1.0	4.951	1.3	0.3229	0.9	0.68
2_17.1	0.02	423	103	122	0.25	1863	15	2046	26	10	2.984	1.0	0.1262	1.5	5.830	1.8	0.3351	1.0	0.54
2_28.1	0.00	86.6	57.8	25.6	0.69	1908	20	1911	25	0	2.902	1.2	0.1170	1.4	5.560	1.8	0.3445	1.2	0.66
2_27.1	0.00	408	143	121	0.36	1913	14	2279	11	19	2.895	0.8	0.1442	0.6	6.871	1.0	0.3455	0.8	0.81
2_20.1	0.00	448	162	135	0.37	1938	13	1921	11	-1	2.852	0.8	0.1177	0.6	5.688	1.0	0.3506	0.8	0.79
2_29.1	0.00	80.5	77.5	25.1	1.00	1994	20	1986	23	0	2.759	1.2	0.1220	1.3	6.100	1.7	0.3624	1.2	0.68
2_3.1	--	801	37.0	294	0.05	2293	18	2727	7.2	19	2.341	0.9	0.1882	0.4	11.09	1.0	0.4273	0.9	0.91
2_4.1	0.00	51.2	57.2	19.6	1.16	2382	32	2350	39	-1	2.237	1.6	0.1504	2.3	9.270	2.8	0.4470	1.6	0.57
2_2.1	0.00	186	209	78.5	1.16	2571	20	2691	11	5	2.041	1.0	0.1842	0.7	12.45	1.2	0.4901	1.0	0.81
2_32.1	0.05	251	15.6	110	0.06	2667	23	2747	9.9	3	1.952	1.0	0.1906	0.6	13.46	1.2	0.5123	1.0	0.87
2_25.1	0.06	403	69.4	183	0.18	2732	18	2708	8.5	-1	1.894	0.8	0.1861	0.5	13.54	1.0	0.5278	0.8	0.85
2_11.1	0.00	202	6.76	96.1	0.03	2834	21	2994	9.3	6	1.811	0.9	0.2219	0.6	16.89	1.1	0.5522	0.9	0.85
2_8.1	0.00	112	40.3	58.6	0.37	3061	29	3082	11	1	1.645	1.2	0.2344	0.7	19.64	1.4	0.6078	1.2	0.86
Sandstone fragments from the Mendeleev Rise, sample AF05-15 (78°58'N, 173°56'W)																			
33.1	0.36	939	784	34.0	0.86	265	10	533	97	101	23.82	3.9	0.0581	4.4	0.336	5.9	0.0420	3.9	0.66
31.1	0.00	495	160	28.7	0.33	421	4.2	390	45	-7	14.82	1.0	0.0545	2.0	0.507	2.3	0.0675	1.0	0.46
20.1	0.10	807	160	48.1	0.21	432	3.9	433	38	0	14.43	0.9	0.0555	1.7	0.530	2.0	0.0693	0.9	0.48
1.1	0.00	249	18.6	34.7	0.08	968	8.3	974	33	1	6.169	0.9	0.0716	1.6	1.599	1.9	0.1621	0.9	0.49
25.1	0.11	479	239	66.9	0.51	969	8.5	962	29	-1	6.166	1.0	0.0712	1.4	1.591	1.7	0.1622	1.0	0.56
17.1	0.00	184	59.1	26.1	0.33	985	10	966	37	-2	6.059	1.1	0.0713	1.8	1.623	2.1	0.1650	1.1	0.53
9.1	0.08	443	191	68.1	0.44	1060	8.6	1086	23	2	5.597	0.9	0.0757	1.2	1.864	1.5	0.1787	0.9	0.61
7.1	0.34	105	40.0	16.5	0.39	1080	13	1098	59	2	5.482	1.3	0.0761	3.0	1.914	3.2	0.1824	1.3	0.39
21.1	0.00	237	81.4	37.7	0.35	1093	12	1105	29	1	5.410	1.2	0.0764	1.5	1.947	1.9	0.1848	1.2	0.64
13.1	0.00	82.0	39.0	13.0	0.49	1096	14	1128	49	3	5.396	1.4	0.0773	2.4	1.974	2.8	0.1853	1.4	0.51
27.1	0.00	190	244	30.8	1.33	1115	12	1100	33	-1	5.297	1.1	0.0762	1.7	1.983	2.0	0.1888	1.1	0.56
5.1	0.08	209	104	35.5	0.52	1165	11	1150	30	-1	5.050	1.0	0.0781	1.5	2.133	1.8	0.1980	1.0	0.56
14.1	0.17	212	140	36.5	0.68	1175	12	1538	33	31	5.000	1.1	0.0955	1.8	2.632	2.1	0.1999	1.1	0.52
30.1	0.00	179	67.3	31.7	0.39	1212	13	1184	32	-2	4.836	1.1	0.0795	1.6	2.266	2.0	0.2068	1.1	0.58
22.1	0.00	154	81.7	29.6	0.55	1299	14	1265	32	-3	4.481	1.2	0.0828	1.6	2.548	2.0	0.2232	1.2	0.58
28.1	0.18	158	107	31.5	0.70	1341	14	1372	36	2	4.322	1.2	0.0875	1.9	2.792	2.2	0.2313	1.2	0.53
4.1	0.05	406	252	91.0	0.64	1493	11	1500	20	0	3.837	0.9	0.0936	1.0	3.363	1.4	0.2606	0.9	0.63
10.1	0.00	164	61.5	37.1	0.39	1508	24	1510	25	0	3.793	1.8	0.0941	1.3	3.421	2.2	0.2636	1.8	0.81
3.1	0.06	239	171	57.9	0.74	1600	13	1636	19	2	3.549	0.9	0.1006	1.0	3.909	1.4	0.2817	0.9	0.67
23.1	0.13	127	69.3	31.6	0.56	1634	17	1635	30	0	3.465	1.2	0.1006	1.6	4.002	2.0	0.2885	1.2	0.60
32.1	--	362	22.4	90.9	0.06	1653	14	1658	19	0	3.421	1.0	0.1018	10	4.105	1.4	0.2924	1.0	0.70
6.1	0.14	131	159	33.1	1.26	1663	16	1627	29	-2	3.398	1.1	0.1002	1.6	4.064	1.9	0.2942	1.1	0.58
16.1	0.05	226	227	58.4	1.04	1698	15	1653	20	-3	3.319	1.0	0.1016	1.1	4.221	1.5	0.3013	1.0	0.68
2.1	--	219	174	58.2	0.82	1741	14	1761	19	1	3.225	1.0	0.1077	1.0	4.606	1.4	0.3101	1.0	0.68
15.1	0.44	220	160	60.0	0.75	1767	16	1753	27	-1	3.168	1.0	0.1072	1.5	4.663	1.8	0.3154	1.0	0.58
24.1	0.00	161	163	47.7	1.05	1911	18	1890	20	-1	2.898	1.1	0.1157	1.1	5.504	1.6	0.3451	1.1	0.70
18.1	0.00	263	208	81.2	0.81	1978	17	2004	27	1	2.785	1.0	0.1232	1.5	6.100	1.8	0.3591	1.0	0.54
29.1	0.00	147	37.3	45.4	0.26	1981	20	2026	21	2	2.779	1.2	0.1248	1.2	6.190	1.6	0.3599	1.2	0.71
19.1	0.04	199	120	63.5	0.63	2037	18	2021	17	-1	2.690	1.0	0.1244	1.0	6.377	1.4	0.3717	1.0	0.73
8.1	0.00	122	31.7	39.3	0.27	2050	20	2038	20	-1	2.671	1.1	0.1257	1.1	6.490	1.6	0.3744	1.1	0.70
34.1	0.00	71.9	40.0	32.5	0.57	2721	31	2747	19	1	1.904	1.4	0.1905	1.2	13.80	1.8	0.5252	1.4	0.77
12.1	0.16	111	80.5	51.6	0.75	2776	26	2758	15	-1	1.857	1.1	0.1919	0.9	14.24	1.5	0.5383	1.1	0.79
11.1	0.12	135	25.0	64.6	0.19	2852	25	2761	14	-3	1.796	1.1	0.1922	0.8	14.75	1.4	0.5566	1.1	0.79
26.1	0.11	102	79.0	51.3	0.80	2979	29	3018	14	1	1.701	1.2	0.2251	0.9	18.24	1.5	0.5875	1.2	0.81
Sandstone fragments from the Mendeleev Rise, sample AF05-20 (77°45'N, 177°30'W)																			
2.1	0.07	346	212	53.0	0.63	1057	4.5	1077	17	2	5.611	0.5	0.0753	0.8	1.850	1.0	0.1782	0.5	0.47
22.1	0.16	148	61.6	23.2	0.43	1080	6.0	1113	28	3	5.483	0.6	0.0767	1.4	1.929	1.5	0.1824	0.6	0.39
8.1	---	168	122	26.8	0.75	1097	7.0	1149	23	5	5.388	0.7	0.0781	1.2	1.998	1.3	0.1856	0.7	0.51
17.1	0.30	229	110	38.2	0.50	1141	5.5	1312	25	15	5.163	0.5	0.0848	1.3	2.266	1.4	0.1937	0.5	0.38
15.1	0.47	33.0	20.3	5.76	0.63	1188	14	1282	83	8	4.942	1.3	0.0835	4.2	2.331	4.4	0.2024	1.3	0.30
11.1	0.96	29.7	8.03	5.27	0.28	1200	15	1206	104	1	4.889	1.4	0.0804	5.3	2.266	5.5	0.2046	1.4	0.26
24.1	0.15	158	86.3	28.2	0.56	1213	7.4	1328	24	9	4.828	0.7	0.0855	1.3	2.442	1.4	0.2071	0.7	0.47
18.1	0.04	170	65.9	31.1	0.40	1245	6.2	1273	21	2	4.692	0.6	0.0832	1.1	2.444	1.2	0.2131	0.6	0.46
1.1	0.41	127	64.0	24.1	0.52	1287	7.4	1400	29	9	4.527	0.6	0.0888	1.5	2.705	1.7	0.2209	0.6	0.38
6.1	0.22	109	69.6	21.4	0.66	1322	7.8	1421	29	7	4.394	0.7	0.0898	1.5	2.817	1.6	0.2276	0.7	0.40
26.1	0.12	162	92.6	31.8	0.59	1329	6.7	1366	22	3	4.369	0.6	0.0872	1.1	2.753	1.3	0.2289	0.6	0.44

Table 1. Continued.

Analysis number	% $^{206}Pb_c$	ppm U	ppm Th	ppm $^{206}Pb^*$	$^{232}Th/^{238}U$	(1) $^{206}Pb/^{238}U$ Age (Ma)	± abs	(1) $^{207}Pb/^{206}Pb$ Age (Ma)	± abs	% Dis.	(1) $^{238}U/^{206}Pb^*$	±%	(1) $^{207}Pb^*/^{206}Pb^*$	±%	(1) $^{207}Pb^*/^{235}U$	±%	(1) $^{206}Pb^*/^{238}U$	±%	err corr
5.1	0.40	49.6	25.7	9.89	0.54	1341	13	1343	51	0	4.323	1.1	0.0862	2.6	2.750	2.8	0.2313	1.1	0.38
9.1	0.07	138	45.5	28.1	0.34	1373	8.4	1390	20	1	4.213	0.7	0.0883	1.0	2.892	1.2	0.2374	0.7	0.54
19.1	0.12	451	162	94.1	0.37	1400	4.4	1460	11	4	4.123	0.3	0.0916	0.6	3.064	0.7	0.2426	0.3	0.51
28.1	0.03	247	107	51.6	0.45	1400	5.7	1444	15	3	4.121	0.5	0.0909	0.8	3.039	0.9	0.2426	0.5	0.50
23.1	0.10	188	74.8	39.6	0.41	1412	6.5	1455	21	3	4.083	0.5	0.0914	1.1	3.086	1.2	0.2449	0.5	0.42
27.1	0.04	96.7	63.1	20.7	0.67	1432	10	1442	22	1	4.021	0.8	0.0908	1.1	3.113	1.4	0.2487	0.8	0.56
7.1	---	186	88.3	40.1	0.49	1443	6.4	1440	16	0	3.985	0.5	0.0907	0.8	3.138	1.0	0.2510	0.5	0.51
4.1	---	126	61.3	27.7	0.50	1476	8.8	1477	19	0	3.886	0.7	0.0925	1.0	3.281	1.2	0.2573	0.7	0.56
20.1	0.04	164	60.9	37.7	0.38	1524	8.3	1667	16	9	3.751	0.6	0.1023	0.9	3.762	1.1	0.2666	0.6	0.58
14.1	0.35	53.1	38.3	12.9	0.74	1596	12	1590	32	0	3.561	0.9	0.0982	1.7	3.801	1.9	0.2808	0.9	0.45
13.1	0.05	115	112	28.2	1.01	1623	10	1658	18	2	3.494	0.7	0.1018	1.0	4.018	1.2	0.2862	0.7	0.59
21.1	0.01	511	227	126	0.46	1624	4.7	1733	8.1	7	3.490	0.3	0.1061	0.4	4.190	0.5	0.2866	0.3	0.59
10.1	0.06	149	75.3	37.8	0.52	1660	7.7	1684	16	1	3.404	0.5	0.1033	0.9	4.183	1.0	0.2938	0.5	0.52
25.1	0.00	149	45.8	38.5	0.32	1697	9.1	1698	15	0	3.320	0.6	0.1041	0.8	4.323	1.0	0.3012	0.6	0.61
16.1	0.00	302	104	84.2	0.36	1813	6.1	1871	9.2	3	3.080	0.4	0.1145	0.5	5.124	0.6	0.3247	0.4	0.60
3.1	0.08	96.2	52.5	28.0	0.56	1877	10	1917	16	2	2.958	0.6	0.1174	0.9	5.472	1.1	0.3381	0.6	0.57
29.1	0.00	258	255	76.3	1.02	1911	7.7	1906	10	0	2.899	0.5	0.1167	0.5	5.551	0.7	0.3450	0.5	0.65
12.1	---	83.7	67.7	37.1	0.84	2685	14	2681	15	0	1.936	0.6	0.1830	0.9	13.04	1.1	0.5166	0.6	0.57
30.1	0.00	40.1	17.7	18.4	0.46	2757	23	2751	18	0	1.873	1.0	0.1910	1.1	14.06	1.5	0.5338	1.0	0.69

Note:
Dots in the first column separate numbers of analyzed grains from numbers of shots.
Errors marked "+/- abs" and "+/- %" are within 1 sigma.
Pb_c and Pb* indicate common and radiogenic lead, respectively.
Columns (1) designate radiogenic Pb calculated using measured ^{204}Pb.
Relative discordancy (% Dis) is calculated as 100 x {[age(207/206)] / [age(206/238)] – 1}.
Error correlation (err corr) is the correlation of errors for Pb/U isotope ratio.

Table 2. U-Pb analytical data obtained by laser ablation coupled with MC-ICPMS-HR NEPTUNE (Thermo TM). Sandstone fragment from the Lomonosov Ridge, sample ALR07-18 (82°30'N, 140°E)

Analysis number	$^{206}Pb/^{238}U$	± 1s, abs	$^{207}Pb/^{206}Pb$	± 1s, abs	$^{206}Pb/^{238}U$ Age (Ma)	± 1s, abs	$^{207}Pb/^{206}Pb$ Age (Ma)	± 1s, abs
1.1	0.2862	0.0032	0.0955	0.0013	1636	21	1533	49
2.1	0.0401	0.0016	0.0630	0.0008	196	17	755	40
3.1	0.1685	0.0066	0.0767	0.0025	878	200	1066	220
4.1	0.1066	0.0011	0.2566	0.0048	662	22	3216	98
5.1	0.1323	0.0062	0.1383	0.0011	568	12	2132	5.3
6.1	0.0618	0.0004	0.0599	0.0011	386	5.6	526	13
7.1	0.3051	0.0026	0.1066	0.0011	1703	33	1709	56
8.1	0.1891	0.0029	0.0793	0.0009	1091	18	1143	21
9.1	0.3257	0.0017	0.1078	0.0002	1832	32	1770	6.8
10.1	0.0302	0.0018	0.0687	0.0012	170	20	818	100
11.1	0.2323	0.0015	0.0794	0.0013	1352	20	1197	35
12.1	0.3223	0.0059	0.1018	0.0008	1840	85	1644	52
13.1	0.3151	0.0013	0.1056	0.0001	1758	28	1729	2.4
14.1	0.1613	0.0096	0.1062	0.0003	933	150	1747	18
15.1	0.1229	0.0057	0.1184	0.0002	689	100	1942	14
16.1	0.3774	0.0061	0.1499	0.0003	2001	88	2334	16
17.1	0.2251	0.0106	0.0958	0.0007	1342	170	1513	38
18.1	0.3328	0.0248	0.1963	0.0041	2001	130	2731	31
19.1	0.0768	0.0010	0.1262	0.0010	479	9.5	2029	9.9
20.1	0.2478	0.0089	0.1084	0.0007	1646	120	1829	22
21.1	0.1918	0.0042	0.0968	0.0044	1169	71	1383	270
22.1	0.2841	0.0014	0.1123	0.0008	1615	29	1820	24
23.1	0.2901	0.0014	0.1061	0.0002	1653	28	1731	13
24.1	0.4707	0.0169	0.1935	0.0008	2376	100	2787	14
25.1	0.1066	0.0011	0.2566	0.0048	1303	76	1652	50
26.1	0.1066	0.0011	0.2566	0.0048	1240	100	1768	14
27.1	0.1176	0.0018	0.1209	0.0003	691	17	1961	5.5
28.1	0.2489	0.0063	0.1052	0.0004	1425	58	1715	7.1
29.1	0.1671	0.0102	0.1194	0.0005	800	30	1953	3.0
30.1	0.4831	0.0035	0.1630	0.0003	2518	56	2502	13
31.1	0.4215	0.0029	0.1548	0.0009	2312	20	2406	37
32.1	0.2801	0.0058	0.1095	0.0002	1587	130	1790	13
33.1	0.1863	0.0060	0.0976	0.0032	1141	97	1501	140
34.1	0.3239	0.0032	0.1964	0.0073	1800	28	2774	90
35.1	0.2673	0.0130	0.1079	0.0010	1379	170	1750	53
36.1	0.0904	0.0015	nd	nd	536	37	nd	nd
37.1	0.2980	0.0031	0.1136	0.0003	1631	26	1861	2.2
38.1	0.2874	0.0010	0.1046	0.0010	1626	23	1725	23
39.1	0.3542	0.0027	0.1150	0.0003	1929	30	1880	6.5
40.1	0.1796	0.0011	0.0761	0.0004	1058	37	1087	35
41.1	0.1908	0.0020	0.0810	0.0022	1126	31	1158	170
42.1	0.2816	0.0138	0.0984	0.0010	1783	130	1655	26
43.1	0.2427	0.0098	0.1129	0.0004	1531	160	1823	25
44.1	0.1549	0.0990	-0.1858	0.4786	583	190	2104	18
45.1	0.3415	0.0036	0.1092	0.0004	1934	44	1770	15
46.1	0.2253	0.0018	0.0972	0.0005	1316	30	1578	56
47.1	0.1134	0.0038	0.0894	0.0007	732	35	1400	21
48.1	0.1867	0.0037	0.1197	0.0002	1161	18	1948	2.7
49.1	0.3046	0.0029	0.1054	0.0003	1740	25	1721	3.1
50.1	0.2865	0.0057	0.1197	0.0006	1614	27	1969	4.3

Note: nd - corresponds to extremely low-Pb content for apropriate estimation of Pb/Pb and U/Pb ratios.

REFERENCES

Akinin, V.V. and E.L. Miller, 2012. Age and Compositional Trends in the Okhotsk-Chukotka Volcanic Belt. In: D.B. Stone, J.G. Clough, D.K. Thurston (compilers): Abstracts of presentations made at ICAM VI, May 30 – June 2, 2011, Fairbanks, Alaska, UAF Geophysical Institute Report UAG-R-335.

Akinin, V.V., J.M. Amato, E.L. Miller, E.Gottlieb and G.O. Polzunenkov, 2012. New Geochronological Data on pre-Mesozoic Rocks (Neoproterozoic to Devonian) from the Arctic Part of the Chukotka Peninsula. In: D.B. Stone, J.G. Clough, D.K. Thurston (compilers): Abstracts of presentations made at ICAM VI, May 30 – June 2, 2011, Fairbanks, Alaska, UAF Geophysical Institute Report UAG-R-335.

Andronikov, A., S. Mukasa, L.A. Mayer, K. Brumley, 2008. First Recovery of Submarine Basalts from the Chukchi Borderland and Alpha/Mendeleev Ridge region, Arctic Ocean. EOS Trans. AGU, 89 (53), Fall Meet. Suppl., Abstract V41D-2124.

Bischof, J.F., D.L. Clark and J.-S.Vincent, 1996. Origin of ice-rafted debris: Pleistocene paleoceanography in the western Arctic Ocean. Paleooceanography, Vol. 11, p. 743-756.

Brumley, K., E.L. Miller, L.A. Mayer, A. Andronikov, J.L. Wooden, T.A. Dumitru, B. Elliott, G.E. Gehrels and S.B. Mukasa, 2010. Petrography and U-Pb detrital zircon geochronology of metasedimentary strata dredged from the Chukchi Borderland, Amerasia Basin, Arctic Ocean. Abstract T31A-2144 presented at 2010 Fall Meeting, AGU, San Francisco, Calif., 13-17 Dec.

Brumley, K., E.L. Miller, L.A. Mayer, J.L. Wooden, T.A. Dumitru, 2011. Petrography and U-Pb zircon geochronology of Caledonian age orthogneisses dredged from the Chukchi Borderland, Arctic Ocean. Abstract T51K-07 presented at 2011 Fall Meeting, AGU, San Francisco, Calif., 5-9 Dec.

Clark, D.L., R.R. Whitman, K.A. Morgan and S.D. Mackey, 1980. Stratigraphy and glaciomarine sediments of the Amerasian Basin, central Arctic Ocean. Spec. Pap. Geol. Soc.Am., 181, p. 1 –57.

Clark, D.L., B.J. Kowallis, L. Gordon Medaris and A.L. Deino, 2000. Orphan Arctic Ocean metasediment clasts: Local derivation from Alpha Ridge or pre-2.6 Ma ice rafting? Geology, v. 28, p. 1143-1146.

Database for ECS Dredge Samples at NOAA/NGDC

Grantz, A., D. Clark, R. Phillips and S. Srivastava, 1998. Fanerozoic stratigraphy of Nortwind Ridge, magnetic anomalies in the Canada Basin and the geometry and timing of rifting in the Amerasia Basin, Arctic Ocean. Geol. Soc. Am. Bull., v. 110, no. 6, p. 801-820.

Grantz, A., V.L. Pease, D.A. Willard, R.L. Phillips and D.L. Clark, 2001. Bedrock cores from 89o North: Implications for the geologic framework and Neogene paleoceanography of Lomonosov Ridge and a tie to the Barents shelf. Geol. Soc. Am. Bull., v. 113, no. 10, p. 1272-1281.

Grantz, A., P.E. Hart and V.A. Childers, 2011a. Geology and tectonic development of the Amerasia and Canada Basins, Arctic Ocean. In: Spencer, A. M., Embry, A. F., Gautier, D. L., Stoupakova, A. V. & Sørensen, K. (eds) Arctic Petroleum Geology. Geological Society, London, Memoirs, v. 35, p. 771-799, doi:10.1144/M35.50.

Grantz, A., R.A. Scott, S.S. Drachev, T.E. Moore and Z.C. Valin, 2011b. Sedimentary successions of the Arctic Region (58o to 90o N) that may be prospective for hydrocarbons. In: Spencer, A. M., Embry, A. F., Gautier, D. L., Stoupakova, A. V. & Sørensen, K. (eds) Arctic Petroleum Geology. Geological Society, London, Memoirs, v.35, p.17–37, doi: 10.1144/M35.2.

Hadlari, T., W.J. Davis, K. Dewing, L.M. Heaman, Y. Lemieux, L. Ootes, B.R. Pratt and L.J. Pyle, 2012. Two detrital zircon signatures for the Cambrian passive margin of northern Laurentia highlighted by new U-Pb results from northern Canada. Geological Society of America Bulletin, v. 124, no. 7-8, p. 1155-1168, doi: 10.1130/B30530.1.

Jackson, H.R., T. Dahl-Jensen and the LORITA working group, 2010. Sedimentary and crustal structure from the Ellesmere Island and Greenland continental shelves onto the Lomonosov Ridge, Arctic Ocean. Geophysical Journal International 182, p. 11–35, doi:

10.1111/j.1365-246X.2010.04604.x
Jokat, W., 2003. Seismic investigations along the western sector of Alpha Ridge, Central Arctic, Ocean. Geophys. J. Int., v. 152, p. 185–201.
Jokat, W., 2009. The expedition of the research vessel “Polarstern” to the Arctic in 2008 (ARK-XXIII/3), Berichte zur Polar- und Meeresforschung (Reports on Polar and Marine Research), Bremerhaven, Alfred Wegener Institute for Polar and Marine Research, 597, 266 pp.
Kaban’kov, V.Ya., I.A. Andreeva, V.N. Ivanov V.N., V.I. Petrova, 2004. The geotectonic nature of the Central Arctic morphostructures and geological implications of bottom sediments for its interpretation. Geotektonika, no. 6, 33-48 (in Russian). English translation: Geotectonics, 2004, vol. 38, part 6, 430-442.
Kaban’kov, V.Ya., I.A. Andreeva, V.V. Krupskaya, D.V. Kaminsky, E.I. Razuvaeva, 2008. New data on the composition and origin of bottom sediments in the southern Mendeleev Ridge, Arctic Ocean. Doklady Akademii Nauk, vol. 419, no. 5, 653–655 (in Russian). English translation: Doklady Earth Sciences, 2008, vol. 419A, no. 3, 403-405.
Kaban’kov, V.Ya., I.A. Andreeva, B.G. Lopatin, 2012. Geology of the Amerasia Sub-Basin. In: Geological-geophysical features of the Arctic Region. Proc. NIIGA-VNIIOkeangeologia, Vol. 223, Ser. 8 (in Russian). In press.
Korago, E.A., A.N. Evdokimov and N.M. Stolbov, 2010. Late Mesozoic mafic magmatism of the northwestern Eurasian continental margin. “VNIIOkeangeologia”, St. Petersburg, 174 pp. (in Russian).
Krylov, A.A., I.A. Andreeva, C. Vogt, J. Backman, V.V. Krupskaya, G.E. Grikurov, K. Moran and H. Shoji, 2008. A shift in heavy and clay mineral provenance indicates a middle Miocene onset of a perennial sea ice cover in the Arctic Ocean. Paleoceanography, v. 23, p. 1-10, PA1S06, doi:10.1029/2007PA001497.
Laverov, N. P., L.I. Lobkovsky, M.V. Kononov, N.L. Dobretsov, V.A. Vernikovsky, S. D. Sokolov and E.V. Shipilov, 2013. A geodynamic model of the evolution of the Arctic Basin and adjacent territories in the Mesozoic and Cenozoic and the outer limit of the Russian continental shelf. Geotectonics, no. 1, p. 1-35 (in Russian).
Miller E.L., J.Toro, G. Gehrels, J.M. Amato, A. Prokopiev, M.I. Tuchkova, V.V. Akinin,T.A. Dumitru, T.E. Moore and M.P. Cecile, 2006. New insights into Arctic paleogeography and tectonics from U-Pb detrital zircon geochronology. Tectonics, v. 25, no. 3, p. 1-19, doi:10.1029/2005TC001830.
Phillips, R.L. and A. Grantz, 2001. Regional variations in provenance and abundance of ice-rafted clasts in Arctic Ocean sediments: implications for the configuration of late Quaternary oceanic and atmospheric circulation in the Arctic. Marine Geology, v. 172, p. 91-115.
Rekant, P.V., M.N. Pyatkova, I.D. Nikolaev and E.E. Taldenkova, 2012. Bottom samples from the Geophysicists Spur as lithological representatives of the Lomonosov Ridge basement (Arctic Ocean). Geology and geoecology of the Euro-Asian continental margins, special issue 4: Geology and mineral resources of the Euro-Asian marginal seas, Moscow, GEOS, p. 29-40 (in Russian).
Van Wagoner, N.A., M. Williamson, P. Robinson and I. Gibson, 1986. First samples of acoustic basement recovered from the Alpha Ridge, Arctic Ocean: new constraints for the origin of the ridge, In: Johnson, G. L. & Kaminuma, K. (eds.) Polar Geophysics. J. Geodyn., v. 6, p. 177-196.
Williams, I.S., 1998. U-Th-Pb Geochronology by Ion Microprobe. In: McKibben, M.A., Shanks III, W.C. and Ridley, W.I. (eds.) Applications of microanalytical techniques to understanding mineralizing processes. Reviews in Economic Geology, v. 7, p. 1-35.